Ann. Henri Poincaré 18 (2017), 559–622
© 2016 Springer International Publishing
1424-0637/17/020559-64
published online October 21, 2016
DOI 10.1007/s00023-016-0525-2

Annales Henri Poincaré

Spectral Theory and Mirror Curves of Higher Genus

Santiago Codesido, Alba Grassi and Marcos Mariño

Abstract. Recently, a correspondence has been proposed between spectral theory and topological strings on toric Calabi–Yau manifolds. In this paper, we develop in detail this correspondence for mirror curves of higher genus, which display many new features as compared to the genus one case studied so far. Given a curve of genus g, our quantization scheme leads to g different trace class operators. Their spectral properties are encoded in a generalized spectral determinant, which is an entire function on the Calabi–Yau moduli space. We conjecture an exact expression for this spectral determinant in terms of the standard and refined topological string amplitudes. This conjecture provides a non-perturbative definition of the topological string on these geometries, in which the genus expansion emerges in a suitable 't Hooft limit of the spectral traces of the operators. In contrast to what happens in quantum integrable systems, our quantization scheme leads to a single quantization condition, which is elegantly encoded by the vanishing of a quantum-deformed theta function on the mirror curve. We illustrate our general theory by analyzing in detail the resolved $\mathbb{C}^3/\mathbb{Z}_5$ orbifold, which is the simplest toric Calabi–Yau manifold with a genus two mirror curve. By applying our conjecture to this example, we find new quantization conditions for quantum mechanical operators, in terms of genus two theta functions, as well as new number-theoretic properties for the periods of this Calabi–Yau.

1. Introduction

It has been conjectured in [1] that there is a precise correspondence between the spectral theory of certain operators and local mirror symmetry. This correspondence postulates that the Weyl quantization of mirror curves to toric Calabi–Yau (CY) threefold leads to trace class operators on $L^2(\mathbb{R})$, and that the spectral determinant of these operators is captured by topological string amplitudes on the underlying CY. As a corollary, one finds an exact quantization condition for their spectrum, in terms of the vanishing of a (deformed)

theta function. The correspondence unveiled in [1] builds upon previous work on the quantization of mirror curves [2,3] and on the relation between supersymmetric gauge theories and quantum integrable systems [4]. It incorporates, in addition, key ingredients from the study of the ABJM matrix model at large N [5–10]. These ingredients are necessary for a fully non-perturbative treatment, beyond the perturbative WKB approach of [3] and of other recent works on the quantization of spectral curves.

The correspondence of [1] between spectral theory and topological strings can be used to give a non-perturbative definition of the standard topological string. The (un-refined) topological string amplitudes appear as quantum mechanical instanton corrections to the spectral problem, and due to their peculiar form, they can be singled out by a 't Hooft-like limit of the so-called fermionic spectral traces of the operator. In addition, using the integral kernel of the operator, which was determined explicitly in [11] in many cases, one can write down a matrix model whose $1/N$ expansion gives exactly the genus expansion of the topological string [12,13]. Therefore, one can regard the correspondence of [1] as a large N Quantum Mechanics/topological string correspondence, with many features of large N gauge/string dualities. In particular, it is a strong/weak duality, since the Planck constant in the quantum mechanical problem, $\hbar$, is identified as the *inverse* string coupling constant.

All the examples of the correspondence that have been studied so far involve local del Pezzo CYs, and their mirror curve has genus one [1,12–14]. It was pointed out in [1] that the relationship between the spectral theory of trace class operators and topological string amplitudes should hold for general toric CYs, i.e., it should hold for mirror curves of arbitrary genus. In this paper, we present a compelling picture for the spectral theory/mirror symmetry correspondence in the higher genus case. This generalization involves some new ingredients. In the theory developed in [1] for the genus one case, the basic object is the spectral determinant of the trace class operator obtained by quantization of the mirror curve. It turns out that a curve of genus g_Σ leads to g_Σ different operators, which are related by explicit transformations.[1] As we show in this paper, there is, nevertheless, a single, generalized spectral determinant, which is an *entire* function on the moduli space of the CY manifold. The spectra of the different operators associated with a higher genus mirror curve are encoded in a *single* quantization condition, which is given, as in [1], by the vanishing of the generalized spectral determinant. This quantization condition can be formulated in an elegant way as the vanishing of a quantum-deformed Riemann theta function on the mirror curve; it determines a family of codimension one submanifolds in moduli space.

The fact that we obtain a single quantization condition from a curve of genus g_Σ might be counter-intuitive to readers familiar with quantum integrable systems, like for example the quantum Toda chain and its generalizations. In those systems, the quantization of the spectral curve leads to g_Σ

[1] In this paper, we will denote by g_Σ the genus of the mirror curve, which should not be confused with the genus g appearing in the genus expansion. The former is a spacetime genus, while the latter is a worldsheet genus.

quantization conditions. This is of course due to the fact that the underlying quantum mechanical system is g_Σ-dimensional, and there are g_Σ commuting Hamiltonians that can (and should) be diagonalized simultaneously. It should be noted, however, that the spectral curve by itself does not carry this additional information. In fact, in the case of quantum mechanical problems on the real line it is quite common that the quantization of a higher genus curve leads to a single quantization condition. This is what happens, for example, for the Schrödinger equation with a confining, polynomial potential of higher degree.

As we have just mentioned, one of the main consequences of the conjecture of [1] is that it provides a non-perturbative definition of topological string theory. This can be also generalized to the higher genus case: as we show in this paper, the generalized spectral determinant leads to fermionic spectral traces $Z(\boldsymbol{N};\hbar)$, depending on g_Σ non-negative integers $\boldsymbol{N} = (N_1, \ldots, N_{g_\Sigma})$. In the 't Hooft limit

$$\hbar \to \infty, \qquad N_i \to \infty, \qquad \frac{N_i}{\hbar} = \lambda_i \quad \text{fixed}, \quad i = 1, \ldots, g_\Sigma, \tag{1.1}$$

these traces have the asymptotic expansion

$$\log Z(\boldsymbol{N};\hbar) \sim \sum_{g \geq 0} \mathcal{F}_g(\boldsymbol{\lambda}) \hbar^{2-2g}, \tag{1.2}$$

where $\mathcal{F}_g(\boldsymbol{\lambda})$ are the genus g free energies of the topological string, in an appropriate conifold frame. In particular, we can regard these fermionic spectral traces, which are completely well-defined objects, as non-perturbative completions of the topological string partition function.

The theory of quantum mirror curves of higher genus is relatively intricate, and we develop it in full detail for what is probably the simplest genus two mirror curve, namely the total resolution of the $\mathbb{C}^3/\mathbb{Z}_5$ orbifold. We perform a detailed study of the associated spectral theory, and in particular we determine the vanishing locus of the spectral determinant on the two-dimensional moduli space, in the so-called maximally supersymmetric case $\hbar = 2\pi$. In addition, we give compelling evidence that the expansion of the topological string free energies near what we call the maximal conifold locus gives the large N expansion of the fermionic spectral traces. This provides a non-perturbative completion of the topological string on this background. As a bonus, we obtain non-trivial identities for the values of the periods of this CY at the maximal conifold locus in terms of the dilogarithm, in the spirit of [15,16].

The organization of this paper is as follows. In Sect. 2, we develop the theory of quantum operators associated with higher genus mirror curves and we construct the appropriate generalization of the spectral determinant. In Sect. 3, we present an explicit, conjectural expression for the spectral determinant in terms of topological string amplitudes, and we explain how the large N limit of the spectral traces provides a non-perturbative definition of the all-genus topological string free energy. In Sect. 4, we test these ideas in detail in the example of the resolved $\mathbb{C}^3/\mathbb{Z}_5$ orbifold. In Sect. 5, we conclude and present some problems for future research. The Appendix summarizes information

about the special geometry of the resolved $\mathbb{C}^3/\mathbb{Z}_5$ orbifold which is needed in Sect. 4.

2. Quantizing Mirror Curves of Higher Genus

2.1. Mirror Curves

In this paper, we will consider mirror curves to toric CY threefold, and we will promote them to quantum operators. Let us first review some well-known facts about local mirror symmetry [17,18] and the corresponding algebraic curves. The toric CY threefold which we are interested in can be described as symplectic quotients,

$$X = \mathbb{C}^{k+3} /\!\!/ G, \tag{2.1}$$

where $G = U(1)^k$. The quotient is specified by a matrix of charges Q_i^α, $i = 0, \ldots, k+2$, $\alpha = 1, \ldots, k$. The CY condition requires the charges to satisfy [19]

$$\sum_{i=0}^{k+2} Q_i^\alpha = 0, \qquad \alpha = 1, \ldots, k. \tag{2.2}$$

The mirrors to these toric CYs were constructed in [17,20,21]. They can be written in terms of $3+k$ complex coordinates $Y^i \in \mathbb{C}^*$, $i = 0, \ldots, k+2$, which satisfy the constraint

$$\sum_{i=0}^{k+2} Q_i^\alpha Y^i = 0, \qquad \alpha = 1, \ldots, k. \tag{2.3}$$

The mirror CY manifold $\widehat{X}$ is given by

$$w^+ w^- = W_X, \tag{2.4}$$

where

$$W_X = \sum_{i=0}^{k+2} x_i \mathrm{e}^{Y_i}. \tag{2.5}$$

The complex parameters x_i, $i = 0, \ldots, k+2$, give a redundant parametrization of the moduli space, and some of them can be set to one. Equivalently, we can consider instead the coordinates

$$z_\alpha = \prod_{i=0}^{k+2} x_i^{Q_i^\alpha}, \qquad \alpha = 1, \ldots, k. \tag{2.6}$$

The constraints (2.3) have a three-dimensional family of solutions. One of the parameters corresponds to a translation of all the coordinates:

$$Y^i \to Y^i + c, \qquad i = 0, \ldots, k+2, \tag{2.7}$$

which can be used for example to set one of the Y^is to zero. The remaining coordinates can be expressed in terms of two variables which we will denote

by x, y. There is still a group of symmetries left, given by transformations of the form [22],

$$\begin{pmatrix} x \\ y \end{pmatrix} \to G \begin{pmatrix} x \\ y \end{pmatrix}, \qquad G \in \mathrm{SL}(2,\mathbb{Z}). \tag{2.8}$$

After solving for the variables Y^i in terms of x, y, one finds a function

$$W_X(\mathrm{e}^x, \mathrm{e}^y), \tag{2.9}$$

which, due to the translation invariance (2.7) and the symmetry (2.8), is only well defined up to an overall factor of the form $\mathrm{e}^{\lambda x+\mu y}$, $\lambda, \mu \in \mathbb{Z}$, and a transformation of the form (2.8). The equation

$$W_X(\mathrm{e}^x, \mathrm{e}^y) = 0 \tag{2.10}$$

defines a Riemann surface Σ embedded in $\mathbb{C}^* \times \mathbb{C}^*$. We will call (2.10) the *mirror curve* to the toric CY threefold X. All the information about the closed string amplitudes on $\widehat{X}$ is encoded in Σ, as shown in [23–25].

The equation of the mirror curve (2.10) can be written down in detail as follows. Given the matrix of charges Q_i^α, we introduce the vectors,

$$\overline{\nu}^{(i)} = \left(1, \nu_1^{(i)}, \nu_2^{(i)}\right), \qquad i = 0, \ldots, k+2, \tag{2.11}$$

satisfying the relations

$$\sum_{i=0}^{k+2} Q_i^\alpha \overline{\nu}^{(i)} = 0. \tag{2.12}$$

In terms of these vectors, the function (2.9) can be written as

$$W_X(\mathrm{e}^x, \mathrm{e}^y) = \sum_{i=0}^{k+2} x_i \exp\left(\nu_1^{(i)} x + \nu_2^{(i)} y\right). \tag{2.13}$$

Clearly, there are many sets of vectors satisfying these constraints, but they differ in reparametrizations and overall factors (as we explained above) and, therefore, they define the same Riemann surface. The genus of this Riemann surface, g_Σ, depends on the toric data, encoded in the matrix of charges, or equivalently in the vectors $\overline{\nu}_i$. Among the parameters (2.6), there will be g_Σ "true" moduli of the geometry, and in addition there will be r_Σ "mass parameters", which lead typically to rational mirror maps (this distinction has been emphasized in [26,27]).

2.2. Quantization

The quantization of mirror curves studied in [1], building on [2,3], is simply based on Weyl quantization of the function (2.9), i.e., the variables x, y are promoted to Heisenberg operators x, y satisfying

$$[\mathsf{x}, \mathsf{y}] = \mathrm{i}\hbar. \tag{2.14}$$

In the genus one case, when the CY is the canonical bundle over a del Pezzo surface S,

$$X = \mathcal{O}(K_S) \to S, \tag{2.15}$$

the function (2.9) can be written in a canonical form, as

$$W_S(\mathrm{e}^x, \mathrm{e}^y) = \mathcal{O}_S(x, y) + u, \tag{2.16}$$

where u is the modulus of the Riemann surface. The quantum operator associated with the toric CY threefold, O_S, is obtained by Weyl quantization of the function $\mathcal{O}_S(x, y)$, and u plays the rôle of (minus) the exponentiated energy, or the fugacity.

The higher genus case is much richer, due to the fact that there are g_Σ different moduli for the curve. As a consequence, there will be g_Σ different "canonical" forms for the curve, which we will write as

$$\mathcal{O}_i(x, y) + \kappa_i = 0, \qquad i = 1, \dots, g_\Sigma. \tag{2.17}$$

Here, κ_i is a modulus of Σ, and in practice it is one of the x_js appearing in (2.13). Of course, the different canonical forms of the curves are related by reparametrizations and overall factors, so we will write

$$\mathcal{O}_i + \kappa_i = \mathcal{P}_{ij} \left(\mathcal{O}_j + \kappa_j \right), \qquad i, j = 1, \dots, g_\Sigma, \tag{2.18}$$

where $\mathcal{P}_{ij}$ is a monomial of the form $\mathrm{e}^{\lambda x + \mu y}$. Equivalently, we can write

$$\mathcal{O}_i = \mathcal{O}_i^{(0)} + \sum_{j \neq i} \kappa_j \mathcal{P}_{ij}. \tag{2.19}$$

We can now perform a standard Weyl quantization of the operators $\mathcal{O}_i(x, y)$. In this way, we obtain g_Σ different operators, which we will denote by O_i, $i = 1, \dots, g_\Sigma$. These operators are Hermitian. The relation (2.18) becomes,

$$\mathsf{O}_i + \kappa_i = \mathsf{P}_{ij}^{1/2} \left(\mathsf{O}_j + \kappa_j \right) \mathsf{P}_{ij}^{1/2}, \qquad i, j = 1, \dots, g_\Sigma, \tag{2.20}$$

where P_{ij} is the operator corresponding to the monomial $\mathcal{P}_{ij}$. In this relation, the "splitting" of P_{ij} in two square roots is due to the fact that we are using Weyl quantization, which leads to Hermitian operators. The expression (2.19) becomes, after promoting both sides to operators,

$$\mathsf{O}_i = \mathsf{O}_i^{(0)} + \sum_{j \neq i} \kappa_j \mathsf{P}_{ij}. \tag{2.21}$$

We can regard the operator $\mathsf{O}_i^{(0)}$ as an "unperturbed" operator, while the moduli κ_j encode different perturbations of it. We will also need,

$$\rho_i^{(0)} = \left(\mathsf{O}_i^{(0)} \right)^{-1}, \qquad i = 1, \dots, g_\Sigma. \tag{2.22}$$

By comparing the coefficients of κ_j in the relation (2.20), we find

$$\mathsf{P}_{ij} = \mathsf{P}_{ji}^{-1} \tag{2.23}$$

and

$$\mathsf{P}_{ik} = \mathsf{P}_{ij}^{1/2} \mathsf{P}_{jk} \mathsf{P}_{ij}^{1/2}, \qquad i \neq k. \tag{2.24}$$

Amusingly, these relationships are a sort of non-commutative version of the the relations between transition functions in the theory of bundles. We will set, by convention,

$$\mathsf{P}_{ii} = 1, \quad i = 1, \dots, g_\Sigma. \tag{2.25}$$

We also have

$$\mathsf{O}_i^{(0)} = \mathsf{P}_{ij}^{1/2} \mathsf{O}_j^{(0)} \mathsf{P}_{ij}^{1/2}. \tag{2.26}$$

Before proceeding, let us examine some examples to illustrate the considerations above.

Example 2.1. *The resolved* $\mathbb{C}^3/\mathbb{Z}_5$ *orbifold.* Let us consider the CY given by the total resolution of the orbifold $\mathbb{C}^3/\mathbb{Z}_5$, where the action has weights $(3,1,1)$. This geometry has been studied in detail in various references, like for example [28–31], and (refined) topological string amplitudes on this background have been recently calculated in [27]. The vectors of charges are given by

$$Q^1 = (-3,1,1,1,0), \quad Q^2 = (1,0,0,-2,1). \tag{2.27}$$

To parametrize the moduli space, we introduce five variables $x_0, \ldots, x_5$, as well as the combinations

$$\begin{aligned} z_1 &= \frac{x_1 x_2 x_3}{x_0^3}, \\ z_2 &= \frac{x_0 x_4}{x_3^2}. \end{aligned} \tag{2.28}$$

A useful choice of vectors for this example is

$$\begin{aligned} \overline{\nu}^{(0)} &= (1,0,0), \\ \overline{\nu}^{(1)} &= (1,1,0), \\ \overline{\nu}^{(2)} &= (1,0,1), \\ \overline{\nu}^{(3)} &= (1,-1,-1), \\ \overline{\nu}^{(4)} &= (1,-2,-2), \end{aligned} \tag{2.29}$$

and the equation for the Riemann surface reads, after setting $x_1 = x_2 = x_4 = 1$,

$$\mathrm{e}^x + \mathrm{e}^y + \mathrm{e}^{-2x-2y} + x_3 \mathrm{e}^{-x-y} + x_0 = 0. \tag{2.30}$$

However, it is easy to see that one can also choose the vectors

$$\begin{aligned} \overline{\nu}^{(0)} &= (1,-1,0), \\ \overline{\nu}^{(1)} &= (1,0,1), \\ \overline{\nu}^{(2)} &= (1,-3,-1), \\ \overline{\nu}^{(3)} &= (1,0,0), \\ \overline{\nu}^{(4)} &= (1,1,0), \end{aligned} \tag{2.31}$$

which leads to the equation

$$\mathrm{e}^x + \mathrm{e}^y + \mathrm{e}^{-3x-y} + x_0 \mathrm{e}^{-x} + x_3 = 0. \tag{2.32}$$

In Fig. 1, we show the vectors ν_i for the system (2.31) (this is sometimes called a height one slice of the fan (2.31)). Of course, although we have chosen the same notations, the variables x, y appearing in (2.32) are not the same ones appearing in (2.30). Rather, they are related by a canonical transformation,

$$-x-y \to x, \qquad 2x+y \to y. \tag{2.33}$$

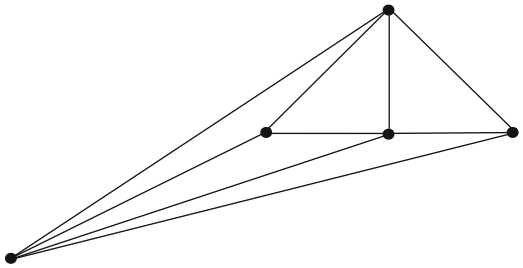

FIGURE 1. A height one slice of the vectors (2.31), providing the toric data for the resolved $\mathbb{C}^3/\mathbb{Z}_5$ orbifold

In this case, the two canonical functions $\mathcal{O}_1(x,y)$ and $\mathcal{O}_2(x,y)$ are given by

$$\begin{aligned}\mathcal{O}_1(x,y) &= \mathrm{e}^{x} + \mathrm{e}^{y} + \mathrm{e}^{-2x-2y} + x_3\mathrm{e}^{-x-y},\\ \mathcal{O}_2(x,y) &= \mathrm{e}^{x} + \mathrm{e}^{y} + \mathrm{e}^{-3x-y} + x_0\mathrm{e}^{-x},\end{aligned} \tag{2.34}$$

and the moduli are

$$\kappa_1 = x_0, \qquad \kappa_2 = x_3. \tag{2.35}$$

In the coordinates appropriate for $\mathcal{O}_1(x,y)$, we have $\mathcal{P}_{12} = \mathrm{e}^{-x-y}$, while in the coordinates appropriate for $\mathcal{O}_2(x,y)$, we have $\mathcal{P}_{21} = \mathrm{e}^{-x}$. In terms of the three-term operators introduced in [11],

$$\mathsf{O}_{m,n} = \mathrm{e}^{\mathsf{x}} + \mathrm{e}^{\mathsf{y}} + \mathrm{e}^{-m\mathsf{x}-n\mathsf{y}}, \tag{2.36}$$

the unperturbed operators are

$$\mathsf{O}_1^{(0)} = \mathsf{O}_{2,2}, \qquad \mathsf{O}_2^{(0)} = \mathsf{O}_{3,1}. \tag{2.37}$$

The theory of the operators (2.36) has been developed in some detail in [11], and it will be quite useful to test some of our results later on. □

Example 2.2. *The resolved $\mathbb{C}^3/\mathbb{Z}_6$ orbifold, or A_2 geometry.* Let us now consider the total resolution of the orbifold $\mathbb{C}^3/\mathbb{Z}_6$, where the action has weights $(4,1,1)$. This is precisely the A_2 geometry studied in the first papers on local mirror symmetry [17,18], which engineers geometrically $SU(3)$ Seiberg–Witten theory. It has also been studied in some detail in [27]. In this case, the charge vectors are

$$\begin{aligned}Q^1 &= (-2,1,0,0,1,0), \qquad Q^2 = (1,-2,1,0,0,0),\\ Q^3 &= (0,0,0,1,-2,1).\end{aligned} \tag{2.38}$$

Like before, we can parametrize the moduli space with six coordinates x_i, $i = 0,\ldots,5$, or in terms of

$$z_1 = \frac{x_1x_4}{x_0^2}, \qquad z_2 = \frac{x_0x_2}{x_1^2}, \qquad z_3 = \frac{x_3x_5}{x_4^2}. \tag{2.39}$$

A useful choice of vectors is,

$$\begin{aligned}\overline{\nu}^{(0)} &= (1,-1,0),\\ \overline{\nu}^{(1)} &= (1,0,0),\end{aligned}$$

$$\begin{aligned}\overline{\nu}^{(2)} &= (1,1,0),\\ \overline{\nu}^{(3)} &= (1,0,1),\\ \overline{\nu}^{(4)} &= (1,-2,0),\\ \overline{\nu}^{(5)} &= (1,-4,-1),\end{aligned} \tag{2.40}$$

and after setting $x_2 = x_3 = x_5 = 1$, we find the curve

$$\mathrm{e}^{x} + \mathrm{e}^{y} + \mathrm{e}^{-4x-y} + x_4\mathrm{e}^{-2x} + x_0\mathrm{e}^{-x} + x_1 = 0. \tag{2.41}$$

The true moduli of the curve are x_0, x_1, while x_4 is a mass parameter. Note that the Batyrev coordinate z_3 depends only on x_4. It is easy to see that there is another realization of the curve above as

$$\mathrm{e}^{2x} + \mathrm{e}^{y} + \mathrm{e}^{-y-2x} + x_4\mathrm{e}^{-x} + x_1\mathrm{e}^{x} + x_0 = 0. \tag{2.42}$$

The canonical operators associated with this geometry can be obtained by Weyl quantization of

$$\begin{aligned}\mathcal{O}_1(x,y) &= \mathrm{e}^{x} + \mathrm{e}^{y} + \mathrm{e}^{-4x-y} + x_4\mathrm{e}^{-2x} + x_0\mathrm{e}^{-x},\\ \mathcal{O}_2(x,y) &= \mathrm{e}^{2x} + \mathrm{e}^{y} + \mathrm{e}^{-y-2x} + x_4\mathrm{e}^{-x} + x_1\mathrm{e}^{x}.\end{aligned} \tag{2.43}$$

They can be regarded as perturbations of $\mathsf{O}_{4,1}$, and of $\mathsf{O}_{1,1}$, respectively. □

It was noted in [1], in the genus one case, that the most interesting operator was not really O_S, but rather its inverse ρ_S. The reason is that ρ_S is expected to be of trace class and positive definite; therefore it has a discrete, positive spectrum, and its Fredholm (or spectral) determinant is well defined. It was rigorously proved in [11] that, in many examples, this is the case, provided the parameters appearing in the operators satisfy certain positivity conditions. In analogy with the genus one case, we expect the operators

$$\rho_i = \mathsf{O}_i^{-1}, \qquad i = 1, \ldots, g_\Sigma \tag{2.44}$$

to exist, be of trace class and positive definite. In the concrete examples that we have considered, this actually follows from the results in [11]. In that paper, it was shown that

$$\rho_{m,n} = \mathsf{O}_{m,n}^{-1} \tag{2.45}$$

exists and is of trace class. It was also shown that the inverse of

$$\mathsf{O}_{m,n} + \mathsf{V}, \tag{2.46}$$

where V is positive and self-adjoint, is also of trace class. Clearly, the operators obtained by Weyl quantization of (2.34) and (2.43) are of this type.

2.3. The Generalized Spectral Determinant

According to the conjecture of [1], when the mirror curve has genus one, many important aspects of the spectral theory of ρ_X can be encoded in the topological string amplitudes on X. We would like to generalize this to mirror curves of higher genus. What are the natural questions that we would like to answer from the point of view of spectral theory? Clearly, we would like to know the spectrum of the operators O_i in terms of enumerative data of X, and in addition, as in [1], we would like to have precise formulae for the

spectral determinants of their inverses ρ_i. However, one should note that, due to (2.20), the operators ρ_i are closely related, and their spectra and spectral determinants are not independent.

In a more fundamental sense, we need an appropriate multivariable generalization of the spectral determinant. In the genus one case, when X is a local del Pezzo of the form (2.15), there is one single modulus κ, and the spectral determinant

$$\Xi_S(\kappa,\hbar) = \det\left(1+\kappa\rho_S\right) \tag{2.47}$$

can be defined in at least three equivalent ways (see [32,33] for a detailed discussion of this issue). The first one is as an infinite product,

$$\Xi_S(\kappa,\hbar) = \prod_{n\geq 0}\left(1+\kappa \mathrm{e}^{-E_n}\right), \tag{2.48}$$

where we denoted the eigenvalues of the positive definite, trace class operator ρ_S by e^{-E_n}, $n=0,1,\ldots$. A more useful definition, advocated by Grothendieck [34] and Simon [32,33], involves the *fermionic spectral traces* $Z_S(N,\hbar)$ defined as

$$Z_S(N,\hbar) = \mathrm{Tr}\left(\Lambda^N(\rho_S)\right), \qquad N=1,2,\ldots \tag{2.49}$$

In this expression, the operator $\Lambda^N(\rho_S)$ is defined by $\rho_S^{\otimes N}$ acting on $\Lambda^N\left(L^2(\mathbb{R})\right)$. A theorem of Fredholm [35] asserts that, if $\rho_S(x_i,x_j)$ is the kernel of ρ_S, the fermionic spectral trace can be computed as a multi-dimensional integral,

$$Z_S(N,\hbar) = \frac{1}{N!}\int \det\left(\rho_S(x_i,x_j)\right)\mathrm{d}^N x. \tag{2.50}$$

The spectral determinant is then given by the convergent series,

$$\Xi_S(\kappa,\hbar) = 1+\sum_{N=1}^{\infty} Z_S(N,\hbar)\kappa^N. \tag{2.51}$$

Another definition of the Fredholm determinant is based on the Fredholm–Plemelj's formula,

$$\Xi_S(\kappa,\hbar) = \exp\left\{-\sum_{\ell=1}^{\infty}\frac{(-\kappa)^\ell}{\ell}\mathrm{Tr}\rho_S^\ell\right\}. \tag{2.52}$$

In the higher genus case, there should exist a generalization of the spectral determinant (2.47), depending on all the moduli $\kappa_1,\ldots,\kappa_{g_\Sigma}$. We also expect to have spectral traces depending on various integers N_i, $i=1,\ldots,g_\Sigma$. One motivation for this comes from the connection between fermionic spectral traces and matrix models developed in [12,13]: in the higher genus case, we expect to have a multi-cut matrix model, and there should be as many cuts as true moduli in the model.

To construct this generalization, we consider the following operators,

$$\mathsf{A}_{jl} = \rho_j^{(0)}\mathsf{P}_{jl}, \quad j,l=1,\ldots,g_\Sigma. \tag{2.53}$$

The operators $\rho_j^{(0)}$ were defined in (2.22), while the operators P_{jl} are defined by (2.20). We will assume that the A_{jl} are of trace class (this can be verified in concrete examples). We now define the *generalized spectral determinant* as

$$\Xi_X(\boldsymbol{\kappa};\hbar) = \det\left(1 + \kappa_1 \mathsf{A}_{j1} + \cdots + \kappa_{g_\Sigma}\mathsf{A}_{jg_\Sigma}\right). \tag{2.54}$$

This definition does not depend on the index j: from the relationships (2.26) and (2.24), we find

$$\mathsf{A}_{il} = \mathsf{P}_{ij}^{-1/2}\mathsf{A}_{jl}\mathsf{P}_{ij}^{1/2}. \tag{2.55}$$

Different choices of the index lead to operators related by a similarity transformation, and their determinants are equal. The generalized spectral determinant (2.54) can be of course regarded as the conventional spectral determinant of the operator

$$\kappa_1 \mathsf{A}_{j1} + \cdots + \kappa_{g_\Sigma}\mathsf{A}_{jg_\Sigma}. \tag{2.56}$$

As shown in [33], if the operators A_{jl} are of trace class, as we are assuming here, (2.54) is *an entire function on the moduli space parametrized by* $\kappa_1, \ldots, \kappa_{g_\Sigma}$. This function can be expanded around the origin $\boldsymbol{\kappa} = 0$ as follows:

$$\Xi_X(\boldsymbol{\kappa};\hbar) = \sum_{N_1\geq 0}\cdots\sum_{N_{g_\Sigma}\geq 0} Z_X(\boldsymbol{N};\hbar)\kappa_1^{N_1}\cdots\kappa_{g_\Sigma}^{N_{g_\Sigma}}, \tag{2.57}$$

with the convention that

$$Z_X(0,\ldots,0;\hbar) = 1. \tag{2.58}$$

This expansion defines the (generalized) fermionic spectral traces $Z_X(\boldsymbol{N};\hbar)$, as promised. These are crucial in our construction, since they will provide a non-perturbative definition of the topological string partition function on X. Fredholm's formula (2.50) can be now used to give an explicit expression for these traces. We have

$$\begin{aligned}\Xi_X(\boldsymbol{\kappa};\hbar) = \sum_{N\geq 0}\frac{1}{N!}\sum_{\sigma\in S_N}(-1)^{\epsilon(\sigma)}\int \mathrm{d}^N x \\ \times\prod_{i=1}^{N}\left(\sum_{\ell}\kappa_\ell A_{j\ell}\left(x_i, x_{\sigma(i)}\right)\right),\end{aligned} \tag{2.59}$$

where S_N is the permutation group of N elements, and we denote by $A_{jl}(x_m, x_n)$ the kernels of the operators defined in (2.53). For fixed $N_1, \ldots N_{g_\Sigma}$ we can count the terms in (2.59) that contribute to

$$\kappa_1^{N_1}\cdots\kappa_{g_\Sigma}^{N_{g_\Sigma}}. \tag{2.60}$$

In particular, this means that we pick up N_i of the A_{ji}. It follows that $Z_X(\boldsymbol{N};\hbar)$ in (2.57) is given by

$$Z_X(\boldsymbol{N};\hbar) = \frac{1}{N_1!\cdots N_{g_\Sigma}!}\int \det_{m,n}\left(R_j(x_m, x_n)\right)\mathrm{d}^N x, \tag{2.61}$$

where

$$N = \sum_{s=1}^{g_\Sigma} N_s, \tag{2.62}$$

and

$$R_j(x_m, x_n) = A_{jl}(x_m, x_n) \quad \text{if} \quad \sum_{s=1}^{l-1} N_s < m \leq \sum_{s=1}^{l} N_s. \tag{2.63}$$

As we showed above, the definition does not depend on the choice of $j = 1, \dots g_\Sigma$. Note that the expansion (2.57) has detailed information about the traces of all the operators A_{ji} and their products.

Let us write some of the above formula in the case $g_\Sigma = 2$, since we will use them later in the paper. In this case, the fermionic spectral traces can be written as

$$\begin{aligned} &Z_X(N_1, N_2; \hbar) \\ &= \frac{1}{N_1! N_2!} \int \det \begin{pmatrix} A_{j1}(x_1, x_1) & \cdots & A_{j1}(x_1, x_N) \\ \vdots & & \vdots \\ A_{j1}(x_{N_1}, x_1) & \cdots & A_{j1}(x_{N_1}, x_N) \\ A_{j2}(x_{N_1+1}, x_1) & \cdots & A_{j2}(x_{N_1+1}, x_N) \\ \vdots & & \vdots \\ A_{j2}(x_N, x_1) & \cdots & A_{j2}(x_N, x_N) \end{pmatrix} \mathrm{d}x_1 \cdots \mathrm{d}x_N. \end{aligned} \tag{2.64}$$

One finds, for example,

$$\begin{aligned} Z_X(1, 1; \hbar) &= \operatorname{Tr} \mathsf{A}_{j1} \operatorname{Tr} \mathsf{A}_{j2} - \operatorname{Tr} (\mathsf{A}_{j1} \mathsf{A}_{j2}) \\ &= \int \mathrm{d}x_1 \mathrm{d}x_2 \, (A_{j1}(x_1, x_1) A_{j2}(x_2, x_2) \\ &\quad - A_{j1}(x_1, x_2) A_{j2}(x_2, x_1)) \,, \end{aligned} \tag{2.65}$$

as well as

$$\begin{aligned} Z_X(2, 1; \hbar) &= \operatorname{Tr} \left(\mathsf{A}_{j1}^2 \mathsf{A}_{j2}\right) - \frac{1}{2} \operatorname{Tr} \left(\mathsf{A}_{j1}^2\right) \operatorname{Tr} \mathsf{A}_{j2} \\ &\quad + \frac{1}{2} \left(\operatorname{Tr} \mathsf{A}_{j1}\right)^2 \operatorname{Tr} \mathsf{A}_{j2} - \operatorname{Tr} \mathsf{A}_{j1} \operatorname{Tr} (\mathsf{A}_{j1} \mathsf{A}_{j2}) \,, \\ Z_X(1, 2; \hbar) &= \operatorname{Tr} \left(\mathsf{A}_{j1} \mathsf{A}_{j2}^2\right) - \frac{1}{2} \operatorname{Tr} \mathsf{A}_{j1} \operatorname{Tr} \left(\mathsf{A}_{j2}^2\right) \\ &\quad + \frac{1}{2} \operatorname{Tr} \mathsf{A}_{j1} \left(\operatorname{Tr} \mathsf{A}_{j2}\right)^2 - \operatorname{Tr} (\mathsf{A}_{j1} \mathsf{A}_{j2}) \operatorname{Tr} \mathsf{A}_{j2}. \end{aligned} \tag{2.66}$$

As we mentioned above, the integral (2.61) should be regarded as a generalized multi-cut matrix model integral.

What is the motivation for the definition (2.54)? We should expect the generalized spectral determinant to contain information about the operators (2.44). To see that this is the case, let us consider the spectral determinant

$$\det (1 + \kappa_1 \rho_1) \,. \tag{2.67}$$

Using Fredholm–Plemelj's formula (2.52), the log of this function can be computed as

$$-\sum_{\ell_1=1}^{\infty}\frac{(-\kappa_1)^{\ell_1}}{\ell_1}\mathrm{Tr}\left(\mathsf{O}_1^{(0)}+\mathsf{P}_1\right)^{-\ell_1}, \tag{2.68}$$

where

$$\mathsf{P}_1=\sum_{j\neq 1}\kappa_j\mathsf{P}_{1j}. \tag{2.69}$$

We first note that

$$\mathrm{Tr}\left(\mathsf{O}_1^{(0)}+\mathsf{P}_1\right)^{-\ell}=\mathrm{Tr}\left[\left(\rho_1^{(0)}\frac{1}{1+\rho_1^{(0)}\mathsf{P}_1}\right)^{\ell}\right]. \tag{2.70}$$

By expanding each denominator in a geometric power series, we find that (2.68) is given by

$$-\sum_{\ell_1\geq 1}\sum_{\ell_2\geq 0}\cdots\sum_{\ell_{g_\Sigma}\geq 0}\frac{1}{\ell_1+\cdots+\ell_{g_\Sigma}}(-\kappa_1)^{\ell_1}\cdots(-\kappa_{g_\Sigma})^{\ell_{g_\Sigma}}\sum_{W\in\mathcal{W}_{\boldsymbol{\ell}}}\mathrm{Tr}(W) \tag{2.71}$$

In this equation,

$$\boldsymbol{\ell}=(\ell_1,\ldots,\ell_{g_\Sigma}) \tag{2.72}$$

and $\mathcal{W}_{\boldsymbol{\ell}}$ is the set of all possible "words" made of ℓ_i copies of the letters A_{1i} defined in (2.53). It is easy to see that (2.71) is almost identical to

$$\begin{aligned}\mathcal{J}_X(\boldsymbol{\kappa};\hbar)&=\log\,\Xi_X(\boldsymbol{\kappa};\hbar)\\&=-\sum_{\ell\geq 1}\frac{(-1)^{\ell}}{\ell}\mathrm{Tr}\left(\kappa_1\mathsf{A}_{11}+\cdots+\kappa_{g_\Sigma}\mathsf{A}_{1g_\Sigma}\right)^{\ell}\\&=-\sum_{\ell_1\geq 0}\sum_{\ell_2\geq 0}\cdots\sum_{\ell_{g_\Sigma}\geq 0}\frac{1}{\ell_1+\cdots+\ell_{g_\Sigma}}(-\kappa_1)^{\ell_1}\cdots(-\kappa_{g_\Sigma})^{\ell_{g_\Sigma}}\\&\quad\times\sum_{W\in\mathcal{W}_{\boldsymbol{\ell}}}\mathrm{Tr}(W),\end{aligned} \tag{2.73}$$

except that all the terms have a strictly positive power of κ_1. It follows that

$$\det\left(1+\kappa_1\rho_1\right)=\frac{\Xi_X(\boldsymbol{\kappa};\hbar)}{\Xi_X((0,\kappa_2,\ldots,\kappa_{g_\Sigma});\hbar)}. \tag{2.74}$$

In addition, a simple inductive argument shows that

$$\begin{aligned}\Xi_X(\boldsymbol{\kappa};\hbar)=\det\left(1+\kappa_1\rho_1\right)&\\\times\det\left(1+\kappa_2\rho_2\Big|_{\kappa_1=0}\right)&\\\cdots\det\left(1+\kappa_{g_\Sigma}\rho_{g_\Sigma}\Big|_{\kappa_1=\cdots=\kappa_{g_\Sigma-1}=0}\right).&\end{aligned} \tag{2.75}$$

In this derivation, we have taken as our starting point the operator ρ_1 and its spectral determinant, but it is clear that we could have used any other operator ρ_i, $i = 1, \ldots, g_\Sigma$. In particular, we have

$$\det(1 + \kappa_i \rho_i) = \frac{\Xi_X(\boldsymbol{\kappa}; \hbar)}{\Xi_X(\kappa_1, \ldots, \kappa_{i-1}, 0, \kappa_{i+1}, \ldots, \kappa_{g_\Sigma}; \hbar)}, \qquad i = 1, \ldots, g_\Sigma. \tag{2.76}$$

If we set all moduli to zero in (2.76), except for κ_i, we find

$$\det\left(1 + \kappa_i \rho_i^{(0)}\right) = \Xi_X(0, \ldots, 0, \kappa_i, 0, \ldots, 0; \hbar), \qquad i = 1, \ldots, g_\Sigma. \tag{2.77}$$

Therefore, the generalized spectral determinant specializes to the spectral determinant of the unperturbed operators appearing in the different canonical forms of the curve. We will see, for example, that the generalized spectral determinant associated with the resolved $\mathbb{C}^3/\mathbb{Z}_5$ geometry gives, after suitable specializations, the spectral determinants of the operators $\rho_{3,1}$ and $\rho_{2,2}$.

The attentive reader has probably noticed that the operators A_{jl} defined in (2.53) are not Hermitian, in general. However, the generalized spectral traces defined by (2.57) are real (for real $\hbar$). This follows immediately from (2.75), which expresses (2.54) as a product of spectral determinants of Hermitian operators.

The generalized spectral determinant (2.54) vanishes in a codimension one submanifold of the moduli space. This submanifold is a global analytic set, since it is determined by the vanishing of an entire function (see [36]). It contains all the required information about the spectrum of the operators ρ_i appearing in the quantization of the mirror curve. For example, it follows from (2.76) that it gives the spectrum of eigenvalues $\mathrm{e}^{-E_n^{(i)}}$ of a given operator ρ_i, as a function of the other moduli κ_j, $j \neq i$. Since this holds for the different operators ρ_k, $k = 1, \ldots, g_\Sigma$, it follows that their spectra are closely related. Heuristically, this can be already seen from (2.20). Let us suppose that $|\psi_n^{(i)}\rangle$ is an eigenstate of O_i, with eigenvalue $\lambda_n^{(i)}$, i.e.,

$$\mathsf{O}_i |\psi_n^{(i)}\rangle = \lambda_n^{(i)} |\psi_n^{(i)}\rangle. \tag{2.78}$$

Note that the operator O_i depends on the moduli κ_l, with $l \neq i$. Then, using (2.20), we find that

$$|\psi_n^{(j)}\rangle = \mathsf{P}_{ij}^{1/2} |\psi_n^{(i)}\rangle \tag{2.79}$$

satisfies

$$\begin{aligned} \mathsf{O}_j |\psi_n^{(j)}\rangle &= \mathsf{O}_j \mathsf{P}_{ij}^{1/2} |\psi_n^{(i)}\rangle \\ &= \mathsf{P}_{ij}^{-1/2} \left(\mathsf{O}_i - \lambda_n^{(i)}\right) |\psi_n^{(i)}\rangle - \kappa_j \mathsf{P}_{ij}^{1/2} |\psi_n^{(i)}\rangle \\ &= -\kappa_j |\psi_n^{(j)}\rangle. \end{aligned} \tag{2.80}$$

The operator O_j depends on the moduli κ_l, with $l \neq j$. For $l \neq i$, the κ_l are the same ones appearing in the operator O_i, while the value of κ_i is $-\lambda_n^{(i)}$. Of course, since $\mathsf{P}_{ij}^{1/2}$ is not bounded, the relation (2.79) only holds if the square

integrability of the wavefunction is not jeopardized. This is the case in the examples that we have looked at, like the resolved $\mathbb{C}^3/\mathbb{Z}_5$ orbifold.

Interestingly, the codimension one submanifold determined by the vanishing of the generalized spectral determinant has been recently proposed as the natural definition of the joint spectrum of the g_Σ-tuple of non-commuting operators $\mathsf{A}_{j1}, \ldots, \mathsf{A}_{jg_\Sigma}$ [36,37].

2.4. Comparison to Quantum Integrable Systems

In the theory that we have developed in the previous sections, the quantization process leads to g_Σ different operators. However, these operators are related by reparametrizations of the coordinates and the relation (2.20). In particular, there is a *single* quantization condition for all of them, given by the vanishing of the generalized spectral determinant (2.54), as in [1]. This vanishing condition selects a discrete family of codimension one submanifolds in the moduli space parametrized by $\kappa_1, \ldots, \kappa_{g_\Sigma}$. We will determine this family in some detail in the case of the $\mathbb{C}^3/\mathbb{Z}_5$ orbifold.

As we mentioned in the Introduction, our quantization scheme might be counter-intuitive for readers familiar with quantum integrable systems, in which the quantization of a genus g_Σ spectral curve leads typically to g_Σ quantization conditions. To appreciate the difference between the two quantization schemes, let us review in some detail the case of the periodic Toda chain of N sites. This system is classically integrable, with $g_\Sigma = N - 1$ Hamiltonians in involution (see [38] for an excellent exposition of the classical chain). In the quantum theory, the Hamiltonians can be diagonalized simultaneously and one obtains in this way g_Σ quantization conditions that determine their spectrum completely [39,40]. An elegant way to obtain the spectrum is using Baxter's equation [41,42], which in the case of the Toda chain is given by,

$$\mathsf{i}^N Q(x + \mathsf{i}\hbar) + \mathsf{i}^{-N} Q(x - \mathsf{i}\hbar) = \Lambda(x) Q(x), \tag{2.81}$$

where

$$\Lambda(x) = x^N - \sum_{j=1}^{N-1} x^{N-1-j} \kappa_j. \tag{2.82}$$

The κ_j can be interpreted as the Hamiltonians of the Toda chain. It was shown in [42] that, by requiring $Q(x)$ to be an *entire* function which decays sufficiently fast at infinity, one recovers the quantization conditions of [39,40].

Baxter's equation can be obtained by formally "quantizing" the spectral curve of the Toda chain, which can be written as

$$2\cosh y = \Lambda(x). \tag{2.83}$$

The conserved Hamiltonians $\kappa_1, \ldots, \kappa_{g_\Sigma}$ are the moduli of the curve. The variables y and x can be regarded as canonically conjugate variables, in which y plays the rôle of the momentum. To quantize (2.83), we promote x, y to Heisenberg operators. In the position representation, we have

$$y \to -\mathsf{i}\hbar \frac{\mathrm{d}}{\mathrm{d}x}. \tag{2.84}$$

If we now regard (2.83) as an operator equation, acting on a wavefunction of the form

$$\psi(x) = \exp\left(\frac{N\pi}{2\hbar}\right) Q(x), \tag{2.85}$$

we recover Baxter's equation (2.81). As already noted by Gutzwiller [39,40], this procedure is purely formal, since the spectral curve (2.83) does not determine by itself the conditions that $Q(x)$ has to satisfy, and one needs additional information. A more detailed analysis [39,40,43,44] shows that this information is provided by the standard $L^2(\mathbb{R}^{g_\Sigma})$ integrability of the original many-body problem, which forces $Q(x)$ to be entire and to decay at infinity in a prescribed way.

The resulting quantization conditions can be also analyzed in a WKB approximation [42]. If we use an ansatz for the wavefunction (2.85) of the form,

$$\psi(x) \sim \exp\left\{-\frac{\mathrm{i}}{\hbar} S(x;\hbar)\right\}, \tag{2.86}$$

where

$$S(x;\hbar) = \sum_{n\geq 0} \hbar^n S_n(x), \tag{2.87}$$

the leading term is determined by $S_0'(x) = y(x)$, where $y(x)$ solves the equation for the spectral curve (2.83), as expected. Based on the all-order WKB solution (2.87), we can define a "quantum" differential as

$$\lambda = \partial_x S(x;\hbar)\mathrm{d}x. \tag{2.88}$$

Analyticity of $Q(x)$ leads to all-order Bohr–Sommerfeld quantization conditions,

$$\oint_{B_i} \lambda = 2\pi\hbar n_i, \qquad i = 1, \ldots, g_\Sigma, \tag{2.89}$$

where B_i are appropriate cycles on the curve (2.83). It was conjectured in [4] that these conditions can be derived from the Nekrasov–Shatashvili (NS) limit of the instanton partition function of $SU(N)$, $\mathcal{N} = 2$ Yang–Mills theory. This limit leads to a quantum-deformed prepotential $\mathcal{F}^{\mathrm{NS}}(\boldsymbol{a};\hbar)$, where $\boldsymbol{a} = (a_1, \ldots, a_{g_\Sigma})$ are flat coordinates parametrizing the Coulomb branch and $g_\Sigma = N - 1$ is the genus of the Seiberg–Witten curve. The conjecture of [4] states that the periods appearing in (2.89) are related to this prepotential by

$$\frac{\partial \mathcal{F}^{\mathrm{NS}}}{\partial a_i} = \oint_{B_i} \lambda, \qquad i = 1, \ldots, g_\Sigma. \tag{2.90}$$

In addition, the flat coordinates a_i are related to the $\kappa_1, \ldots, \kappa_{g_\Sigma}$ through a "quantum" mirror map,

$$a_i = \oint_{A_i} \lambda, \qquad i = 1, \ldots, g_\Sigma, \tag{2.91}$$

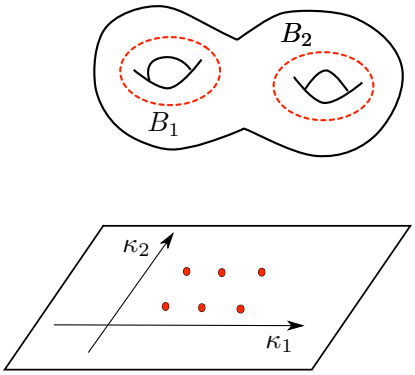

FIGURE 2. In the quantum Toda lattice, the quantum spectral curve leads to $g_\Sigma = N-1$ quantization conditions, which select an infinite set of points in the moduli space parametrized by $\kappa_1, \dots, \kappa_{g_\Sigma}$. We show a *cartoon* of this situation in the case $g_\Sigma = 2$, which should be compared to the actual calculation in Figure 4 of [48]

where A_i are appropriate cycles on the spectral curve. This conjecture was verified, in the very first orders of the perturbative WKB expansion, in [45,46]. Additional evidence for this claim has been also provided in for example [47].

Therefore, in the case of quantum integrable systems of the Toda type, one has g_Σ quantization conditions, which in the all-order WKB quantization can be written as in (2.89). The solution to these conditions on the g_Σ-dimensional moduli space parametrized by the Hamiltonians $\kappa_1, \dots, \kappa_{g_\Sigma}$ is a set of points, i.e., a submanifold of codimension g_Σ. In Fig. 2, we show a cartoon of how the quantization conditions, in the case of $g_\Sigma = 2$, lead to such a discrete spectrum. This cartoon should be compared to Figure 4 of [48], which shows the result of the actual calculation.

As we already noted, the quantum version of the Toda spectral curve does not lead by itself to a well-defined spectral problem: one needs additional conditions that follow from a detailed analysis of the original integrable system, which has g_Σ Hamiltonians in involution and requires g_Σ quantization conditions. However, this does not mean that a curve of genus g_Σ should always lead, after quantization, to g_Σ quantization conditions. The simplest example showing that this is not the case is a one-dimensional particle in an (even) confining potential, with a classical Hamiltonian

$$H(x,y) = \frac{y^2}{2} + V(x), \qquad V(x) = x^{2N} + c_{N-1}x^{2(N-2)} + \cdots + c_0. \quad (2.92)$$

The curve

$$H(x,y) = E \quad (2.93)$$

has genus $g_\Sigma = N-1$. The "quantization" of this curve leads to a standard eigenvalue problem for a Schrödinger equation with potential $V(x)$. For real c_i,

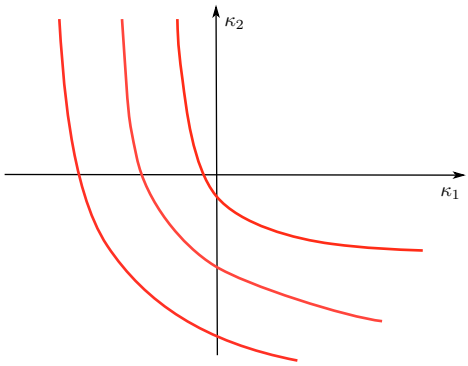

FIGURE 3. The quantization of a higher genus mirror curve leads to a *single* quantization condition, which defines a discrete family of codimension one submanifolds in moduli space. Here, the κ_i should be understood as $-\mathrm{e}^{E_i}$, where E_i are the energies. This *cartoon* should be compared to the actual calculation for the resolved $\mathbb{C}^3/\mathbb{Z}_5$ geometry and $\hbar = 2\pi$, in Fig. 5

$i = 0, \ldots, N-1$, the spectrum is real and discrete, and there should be a single quantization condition, expressing the energy E as a function of the parameter c_i and the quantum number n. Semiclassically, and for E sufficiently large, the quantization condition is simply given by the Bohr–Sommerfeld rule,

$$\oint_B y(x)\mathrm{d}x = 2\pi\hbar n, \qquad n = 0, 1, \ldots, \tag{2.94}$$

where B is the cycle associated with the turning points of the classical motion. Therefore, although the curve (2.92) has genus $N-1$, when interpreted as describing a particle in an even, confining potential, its quantum version should lead to a single quantization condition, associated with the preferred cycle B. One could think that the other cycles of the higher genus curve do not play a rôle. However, this is not so. The reason is that, in the exact WKB method, one should consider complex trajectories around all possible cycles of the underlying curve, and these trajectories will lead to complex instanton corrections to (2.94), as first pointed out in the seminal paper [49,50].

The quantization of higher genus mirror curves considered in this paper is in fact very similar to the quantization of the curve (2.93): there is in principle no need to specify g_Σ quantization conditions, since (at least in the cases we have considered) the relevant operators O_i have a well-defined discrete, positive spectrum which is determined by a single quantization condition. This condition determines a discrete family of codimension one submanifolds in moduli space. A cartoon for what we expect when $g_\Sigma = 2$ is shown in Fig. 3. At the same time, our quantization scheme leads to a genuine g_Σ-dimensional problem, as reflected in the fact that we have g_Σ different operators and our generalized fermionic spectral traces depend on g_Σ different integers. Our goal

will be to determine the quantization condition, as well as the generalized spectral determinant (2.54) and spectral traces, from the topological string amplitudes on X. The cartoon in Fig. 3 can be compared to the actual calculation of such a family in the example of the resolved $\mathbb{C}^3/\mathbb{Z}_5$ geometry, and for $\hbar = 2\pi$ in Fig. 5.

3. Spectral Determinants and Topological Strings

3.1. A Conjecture for the Generalized Spectral Determinant

We will now state our main conjecture, which generalizes [1] to the higher genus case, and provides an explicit expression for the generalized spectral determinant (2.54) in terms of topological string amplitudes. As in [1], the key object is the (modified) grand potential introduced in [9].

To state the conjecture, let us first recall some basic geometric ingredients. As we noted above, in the geometry there are g_Σ moduli, κ_i, $i = 1, \ldots, g_\Sigma$, and r_Σ mass parameters, ξ_j, $j = 1, \ldots, r_\Sigma$. We will also parametrize the moduli through the "chemical potentials" μ_i, defined by

$$\kappa_i = \mathrm{e}^{\mu_i}, \qquad i = 1, \ldots, g_\Sigma. \tag{3.1}$$

The Batyrev coordinates z_i can be written as

$$-\log z_i = \sum_{j=1}^{g_\Sigma} C_{ij}\mu_j + \sum_{k=1}^{r_\Sigma} \alpha_{ik} \log \xi_k, \qquad i = 1, \ldots, g_\Sigma + r_\Sigma. \tag{3.2}$$

The coefficients C_{ij} determine a $(g_\Sigma + r_\Sigma) \times g_\Sigma$ matrix which can be read off from the toric data of X. It is possible to choose the Batyrev coordinates in such a way that, for $i = 1, \ldots, g_\Sigma$, the z_is correspond to true moduli, while for $i = g_\Sigma + 1, \ldots, g_\Sigma + r_\Sigma$, they correspond to mass parameters. For such a choice, the non-vanishing coefficients

$$C_{ij}, \quad i, j = 1, \ldots, g_\Sigma, \tag{3.3}$$

form an invertible matrix, which agrees (up to an overall sign) with the charge matrix C_{ij} appearing in [27]. The classical mirror map expresses the large radius, Kähler parameters t_i of the CY in terms of the Batyrev coordinates z_i. As first shown in [3], the classical mirror map can be promoted to a *quantum* mirror map $t_i(\hbar)$ which depends now on $\hbar$. Explicit expressions for the quantum mirror map can be obtained in various ways, see for instance [51,52] for examples.

In addition to the quantum mirror map, we need various enumerative ingredients from topological string theory. First of all, we need the conventional genus g free energies $F_g(\mathbf{t})$ of X, $g \geq 0$, in the so-called large radius frame. These free energies are given by a "classical" or perturbative part, plus a series of worldsheet instanton corrections which can be regarded as generating functionals for the Gromov–Witten invariants of X. The genus zero free energy is given by

$$F_0(\mathbf{t}) = \frac{1}{6} a_{ijk} t_i t_j t_k + \sum_{\mathbf{d}} N_0^{\mathbf{d}} \mathrm{e}^{-\mathbf{d}\cdot\mathbf{t}}. \tag{3.4}$$

At genus one, one has

$$F_1(\mathbf{t}) = b_i t_i + \sum_{\mathbf{d}} N_1^{\mathbf{d}} \mathrm{e}^{-\mathbf{d}\cdot\mathbf{t}}, \tag{3.5}$$

while at higher genus one finds

$$F_g(\mathbf{t}) = C_g + \sum_{\mathbf{d}} N_g^{\mathbf{d}} \mathrm{e}^{-\mathbf{d}\cdot\mathbf{t}}, \qquad g \geq 2. \tag{3.6}$$

In these formulae, $N_g^{\mathbf{d}}$ are the Gromov–Witten invariants of X at genus g and multi-degree $\mathbf{d}$. The coefficients a_{ijk}, b_i in (3.4), (3.5) are cubic and linear couplings characterizing the perturbative genus zero and genus one free energies, while C_g in (3.6) is the so-called constant map contribution [53]. The total free energy of the topological string is defined as the formal series,

$$\begin{aligned} F^{\mathrm{WS}}(\mathbf{t}, g_s) &= \sum_{g\geq 0} g_s^{2g-2} F_g(\mathbf{t}) \\ &= F^{(\mathrm{p})}(\mathbf{t}, g_s) + \sum_{g\geq 0} \sum_{\mathbf{d}} N_g^{\mathbf{d}} \mathrm{e}^{-\mathbf{d}\cdot\mathbf{t}} g_s^{2g-2}, \end{aligned} \tag{3.7}$$

where

$$F^{(\mathrm{p})}(\mathbf{t}, g_s) = \frac{1}{6 g_s^2} a_{ijk} t_i t_j t_k + b_i t_i + \sum_{g\geq 2} C_g g_s^{2g-2} \tag{3.8}$$

and g_s is the topological string coupling constant. As it is well known [54], the sum over Gromov–Witten invariants in (3.7) can be resummed order by order in $\exp(-t_i)$, at all orders in g_s. This resummation involves a new set of enumerative invariants, the so-called Gopakumar–Vafa (GV) invariants $n_g^{\mathbf{d}}$. Out of these invariants, one constructs the generating series

$$F^{\mathrm{GV}}(\mathbf{t}, g_s) = \sum_{g\geq 0} \sum_{\mathbf{d}} \sum_{w=1}^{\infty} \frac{1}{w} n_g^{\mathbf{d}} \left(2 \sin \frac{w g_s}{2}\right)^{2g-2} \mathrm{e}^{-w\mathbf{d}\cdot\mathbf{t}}, \tag{3.9}$$

and one has, as an equality of formal series,

$$F^{\mathrm{WS}}(\mathbf{t}, g_s) = F^{(\mathrm{p})}(\mathbf{t}, g_s) + F^{\mathrm{GV}}(\mathbf{t}, g_s). \tag{3.10}$$

One can generalize the Gopakumar–Vafa invariants to define the so-called *refined BPS invariants* [55–57]. These invariants depend on the degrees $\mathbf{d}$ and on two non-negative half-integers, j_L, j_R. We will denote them by $N_{j_L,j_R}^{\mathbf{d}}$, and they are also integers. The Gopakumar–Vafa invariants are particular combinations of these refined BPS invariants, and one has the following relationship between generating functionals,

$$\sum_{j_L, j_R} \chi_{j_L}(q)(2j_R+1) N_{j_L,j_R}^{\mathbf{d}} = \sum_{g\geq 0} n_g^{\mathbf{d}} \left(q^{1/2} - q^{-1/2}\right)^{2g}, \tag{3.11}$$

where q is a formal variable and

$$\chi_j(q) = \frac{q^{2j+1} - q^{-2j-1}}{q - q^{-1}} \tag{3.12}$$

is the $SU(2)$ character for the spin j. We note that the sums in (3.11) are well defined, since for given degrees $\mathbf{d}$ only a finite number of j_L, j_R, g give a non-zero contribution. Out of these refined BPS invariants, one can define the so-called NS free energy,

$$F^{\mathrm{NS}}(\mathbf{t}, \hbar) = \frac{1}{6\hbar} a_{ijk} t_i t_j t_k + b_i^{\mathrm{NS}} t_i \hbar + \sum_{j_L, j_R} \sum_{w, \mathbf{d}} N^{\mathbf{d}}_{j_L, j_R} \frac{\sin \frac{\hbar w}{2}(2j_L+1) \sin \frac{\hbar w}{2}(2j_R+1)}{2w^2 \sin^3 \frac{\hbar w}{2}} \mathrm{e}^{-w \mathbf{d}\cdot\mathbf{t}}. \tag{3.13}$$

In this equation, the coefficients a_{ijk} are the same ones that appear in (3.4), while b_i^{NS} can be obtained using mirror symmetry as in [58]. This generating functional involves a particular combination of the refined BPS invariants, which defines the NS limit of the refined topological string. The NS limit was first discussed in the context of gauge theory in [4]. By expanding (3.13) in powers of $\hbar$, we find the NS free energies at order n,

$$F^{\mathrm{NS}}(\mathbf{t}, \hbar) = \sum_{n=0}^{\infty} F_n^{\mathrm{NS}}(\mathbf{t}) \hbar^{2n-1}, \tag{3.14}$$

and the expression (3.13) can be regarded as a Gopakumar–Vafa-like resummation of the series in (3.14). We recall that the first term in this series, $F_0^{\mathrm{NS}}(\mathbf{t})$, is equal to $F_0(\mathbf{t})$, the standard genus zero free energy. Note that the term involving the coefficients b_i^{NS} contributes to $F_1^{\mathrm{NS}}(\mathbf{t})$.

With all these ingredients, we are ready to define, following [9], the so-called *modified grand potential* of the CY X. It is the sum of two functions. The first one is

$$\begin{aligned} \mathsf{J}_X^{\mathrm{WKB}}(\boldsymbol{\mu}, \boldsymbol{\xi}, \hbar) = {} & \frac{t_i(\hbar)}{2\pi} \frac{\partial F^{\mathrm{NS}}(\mathbf{t}(\hbar), \hbar)}{\partial t_i} \\ & + \frac{\hbar^2}{2\pi} \frac{\partial}{\partial \hbar} \left(\frac{F^{\mathrm{NS}}(\mathbf{t}(\hbar), \hbar)}{\hbar} \right) \\ & + \frac{2\pi}{\hbar} b_i t_i(\hbar) + A(\boldsymbol{\xi}, \hbar). \end{aligned} \tag{3.15}$$

Note that, in the second term, the derivative w.r.t. $\hbar$ does not act on the implicit dependence of $t_i(\hbar)$ (it is a true partial derivative). The function $A(\boldsymbol{\xi}, \hbar)$ is not known in closed form for arbitrary geometries, although detailed conjectures for its form exist in some cases. It is closely related to a resummed form of the constant map contribution appearing in (3.6). The function (3.15) is perturbative in $\hbar$, and it can be in principle obtained by performing a resummation of the all-order WKB expansion, hence its name. At leading order in $\hbar$, the quantum mirror map becomes the classical mirror map $t_i(\hbar) \approx t_i$, and

$$\mathsf{J}_X^{\mathrm{WKB}}(\boldsymbol{\mu}, \boldsymbol{\xi}, \hbar) = \frac{1}{\hbar} \mathsf{J}_0^X(\boldsymbol{\mu}, \boldsymbol{\xi}) + \cdots, \tag{3.16}$$

where

$$\mathsf{J}_0^X(\boldsymbol{\mu},\boldsymbol{\xi}) = \frac{1}{2\pi}\left(t_i\frac{\partial F_0}{\partial t_i} - 2F_0\right) + 2\pi b_i t_i \tag{3.17}$$

and F_0 is the genus zero free energy.

The second function is the "worldsheet" modified grand potential, which is obtained from the generating functional (3.9),

$$\mathsf{J}_X^{\mathrm{WS}}(\boldsymbol{\mu},\boldsymbol{\xi},\hbar) = F^{\mathrm{GV}}\left(\frac{2\pi}{\hbar}\mathbf{t}(\hbar) + \pi\mathrm{i}\mathbf{B}, \frac{4\pi^2}{\hbar}\right). \tag{3.18}$$

It involves a constant vector $\mathbf{B}$ (or "B-field") which depends on the geometry under consideration. This vector should satisfy the following requirement: for all $\mathbf{d}$, j_L and j_R such that $N^{\mathbf{d}}_{j_L,j_R}$ is non-vanishing, we must have

$$(-1)^{2j_L+2j_R+1} = (-1)^{\mathbf{B}\cdot\mathbf{d}}. \tag{3.19}$$

For local del Pezzo CY threefold, the existence of such a vector was established in [9]. Note that the effect of this constant vector is to replace

$$\mathrm{e}^{-\mathbf{t}} \to \mathrm{e}^{-\mathbf{t}-\pi\mathrm{i}\mathbf{B}} \tag{3.20}$$

in the generating functional (3.9). Note as well that the string coupling constant g_s is related to the Planck constant of the spectral problem by

$$g_s = \frac{4\pi^2}{\hbar}. \tag{3.21}$$

Therefore, the strong string coupling regime corresponds to the semiclassical limit of the spectral problem, while the weakly coupled regime of the topological string corresponds to a highly quantum regime in the spectral problem.

The *total, modified grand potential* is the sum of the above two functions,

$$\mathsf{J}_X(\boldsymbol{\mu},\boldsymbol{\xi},\hbar) = \mathsf{J}_X^{\mathrm{WKB}}(\boldsymbol{\mu},\boldsymbol{\xi},\hbar) + \mathsf{J}_X^{\mathrm{WS}}(\boldsymbol{\mu},\boldsymbol{\xi},\hbar), \tag{3.22}$$

and it was first considered in [9]. When the mirror curve has genus one, it agrees with the modified grand potential of [1], although we have written it in a slightly different way. In particular, the modified grand potential of [1] involves a perturbative part, a membrane part, and a worldsheet part. Here, we have put together the perturbative and the membrane part in the WKB grand potential. The quantity (3.22) has the following structure,

$$\begin{aligned}\mathsf{J}_X(\boldsymbol{\mu},\boldsymbol{\xi},\hbar) = {} & \frac{1}{12\pi\hbar}a_{ijk}t_i(\hbar)t_j(\hbar)t_k(\hbar) \\ & + \left(\frac{2\pi b_i}{\hbar} + \frac{\hbar b_i^{\mathrm{NS}}}{2\pi}\right)t_i(\hbar) \\ & + \mathcal{O}\left(\mathrm{e}^{-t_i(\hbar)}, \mathrm{e}^{-2\pi t_i(\hbar)/\hbar}\right).\end{aligned} \tag{3.23}$$

The last term stands for a formal power series in $\mathrm{e}^{-t_i(\hbar)}$, $\mathrm{e}^{-2\pi t_i(\hbar)/\hbar}$, whose coefficients depend explicitly on $\hbar$. However, this series is *a priori* ill defined when $\hbar$ is a rational multiple of π. This is due to the double poles in the trigonometric functions appearing in (3.13) and (3.9). However, although the generating functionals (3.15) and (3.18) diverge separately, the poles cancel

in the sum [9], as in the HMO cancellation mechanism discovered in [7]. The presence of a B-field satisfying (3.19) is crucial for this cancellation. In the higher genus case, we have established the existence of such a $\mathbf{B}$ in the examples we have studied. Clearly, it would be important to determine $\mathbf{B}$ in full generality for any toric geometry. Note that, in addition, our expression for (3.22) is, as in [1], intrinsically a large radius expansion. We note that only at large radius we have geometric tools to sum up the $\hbar$ corrections at all orders.

After introducing all of our ingredients, we are ready to state our main conjecture. We claim that the generalized spectral determinant (2.54) is given by

$$\Xi_X(\boldsymbol{\kappa};\hbar) = \sum_{\mathbf{n}\in\mathbb{Z}^{g_\Sigma}} \exp\left(\mathsf{J}_X(\boldsymbol{\mu}+2\pi\mathrm{i}\mathbf{n},\boldsymbol{\xi},\hbar)\right). \tag{3.24}$$

It is understood that the generalized spectral determinant also depends on the mass parameters $\boldsymbol{\xi}$, but we will not write this dependence explicitly. As in [1], the right-hand side of (3.24) defines a quantum-deformed (or generalized) Riemann theta function by

$$\Xi_X(\boldsymbol{\kappa};\hbar) = \exp\left(\mathsf{J}_X(\boldsymbol{\mu},\boldsymbol{\xi},\hbar)\right)\Theta_X(\boldsymbol{\kappa};\hbar). \tag{3.25}$$

We note that the function $A(\boldsymbol{\xi},\hbar)$ appearing in (3.15) can be fixed by requiring that the expansion of the generalized spectral determinant around $\boldsymbol{\kappa}=0$ starts with 1. The expression (3.24) looks rather formal, but in fact it can be computed systematically (for arbitrary $\hbar$) near the large radius point of moduli space, as shown in [1] in the genus one case. Interestingly, if our conjecture is true, the resulting expression is in fact an *analytic* function on the CY moduli space. This is surprising, since the modified grand potential (3.22) is not analytic. However, the inclusion of the quantum theta function should cure the lack of analyticity. This is related to the observation in [59] that including generalized theta functions in the total partition functions restores modular invariance. Note though that, in contrast to what happened in [59], the quantum theta function appearing in (3.25) is well defined, at least as an asymptotic expansion. In addition, and as we will see in the next section, when $\hbar=2\pi$, the quantum theta function becomes a perfectly well defined, ordinary theta function.

3.2. The Maximally Supersymmetric Case

As in the genus one case, an important simplification in the above formulae occurs when $\hbar=2\pi$. In this case, the contribution to (3.9) involving invariants with $g\geq 2$ vanishes. After carefully canceling the poles, one finds that (3.22) becomes

$$\begin{aligned}\mathsf{J}_X(\boldsymbol{\mu},\boldsymbol{\zeta},\hbar) = \frac{1}{4\pi^2}\left\{\frac{1}{2}\sum_{i,j=1}^{g_\Sigma+r_\Sigma} t_i t_j \frac{\partial^2\widehat{F}_0}{\partial t_i\partial t_j} - \sum_{i=1}^{g_\Sigma+r_\Sigma} t_i\frac{\partial\widehat{F}_0}{\partial t_i} + \widehat{F}_0\right\} \\ + \widehat{F}_1 + \widehat{F}_1^{\mathrm{NS}}.\end{aligned} \tag{3.26}$$

In these formulae, the generating functionals $\widehat{F}_0$, $\widehat{F}_1$ and $\widehat{F}_1^{\mathrm{NS}}$ are the same ones appearing in (3.4), (3.5), (3.14), but where we perform the replacement

(3.20) in the instanton expansion (i.e., we do not make such a replacement in the polynomial terms in $\mathbf{t}$.) In (3.26), t_i denotes the quantum mirror map evaluated at $\hbar = 2\pi$. It turns out that this equals the classical mirror map, up to a change of sign in the expansion in the moduli. This change of sign is precisely the one that would lead to (3.20).

As a consequence of this simplification, the quantum-deformed theta function becomes

$$\Theta_X(\boldsymbol{\kappa}; 2\pi) = \sum_{\mathbf{n}\in\mathbb{Z}^{g_\Sigma}} \exp\left[\pi \mathrm{i}^t \mathbf{n}\tau\mathbf{n} + 2\pi\mathrm{i}\mathbf{n}\cdot\boldsymbol{\upsilon} - \frac{\mathrm{i}\pi}{3} a_{ijk} C_{il} C_{jm} C_{kp} n_l n_m n_p\right]. \tag{3.27}$$

In this equation, τ is a $g_\Sigma \times g_\Sigma$ matrix given by

$$\tau_{lm} = -\frac{1}{2\pi\mathrm{i}} C_{jl} C_{km} \frac{\partial^2 \widehat{F}_0}{\partial t_j \partial t_k}, \qquad l, m = 1, \ldots, g_\Sigma, \tag{3.28}$$

where the sum over k, j runs from 1 to $g_\Sigma + r_\Sigma$. As explained in [27], this is nothing but the τ matrix of the mirror curve. It is a symmetric matrix satisfying

$$\mathrm{Im}(\tau) > 0. \tag{3.29}$$

In addition, the vector $\boldsymbol{\upsilon}$ appearing in (3.27) has components

$$\upsilon_m = \frac{C_{jm}}{4\pi^2}\left\{\frac{\partial^2 \widehat{F}_0}{\partial t_j \partial t_k} t_k - \frac{\partial \widehat{F}_0}{\partial t_j}\right\} + C_{jm}\left(b_j + b_j^{\mathrm{NS}}\right), \qquad m = 1, \ldots, g_\Sigma \tag{3.30}$$

where the sum over k, j runs over all the $g_\Sigma + r_\Sigma$ indices. In all the examples we have considered, the cubic terms in (3.27) can be traded by quadratic or linear terms. This adds constant, real shifts to τ and $\boldsymbol{\upsilon}$. The resulting matrix and vector will be denoted by $\widetilde{\tau}$ and $\widetilde{\boldsymbol{\upsilon}}$. In this way, (3.27) becomes (up to an overall constant) a conventional higher genus Riemann–Siegel theta function on Σ, which we will write as

$$\Theta_X(\boldsymbol{\kappa}; 2\pi) = \sum_{\mathbf{n}\in\mathbb{Z}^g} \exp\left[\pi \mathrm{i}^t \mathbf{n}\widetilde{\tau}\mathbf{n} + 2\pi\mathrm{i}\mathbf{n}\cdot\widetilde{\boldsymbol{\upsilon}}\right]. \tag{3.31}$$

Note that $\mathrm{Im}\,(\widetilde{\tau}) = \mathrm{Im}\,(\tau)$; therefore, the theta function (3.31) is still well defined. This result is a direct generalization of the genus one case considered in [1].

As we have discussed, the quantization condition for the operators associated with X is obtained by looking at the vanishing locus of the generalized spectral determinant. In the maximally supersymmetric case, this has a beautiful interpretation. The vanishing locus of (3.31) on the Jacobi torus is by definition the *theta divisor* D_Θ. The period $\widetilde{\boldsymbol{\upsilon}}$ can be regarded as a map from the moduli space $\mathcal{M}$ parametrized by $\boldsymbol{\kappa}$, to the Jacobi torus,

$$\widetilde{\boldsymbol{\upsilon}} : \mathcal{M} \to \mathbb{T}^{2g_\Sigma}. \tag{3.32}$$

It follows that the vanishing locus giving the quantization condition can be geometrically interpreted as the inverse image of the theta divisor by the map $\widetilde{\boldsymbol{\upsilon}}$:

$$\widetilde{\boldsymbol{\upsilon}}^{-1}\left(D_\Theta\right) \subset \mathcal{M}. \tag{3.33}$$

Of course, the same interpretation can be made in the genus one case. In the generic case, one has to consider the quantum-deformed theta function, and its vanishing locus will be a quantum deformation of the locus above.

3.3. Spectral Traces at Large N and Non-perturbative Topological Strings

One of the most surprising consequences of the correspondence between spectral theory and mirror symmetry is that the *conventional* topological string can be obtained from a 't Hooft-like limit of the fermionic spectral traces. In the case of genus one curves, this was explained in detail in [12]. First of all, note that these traces, which appear as coefficients in the expansion (2.57), can be written as

$$Z_X(\boldsymbol{N};\hbar) = \frac{1}{(2\pi\mathrm{i})^{g_\Sigma}} \oint_0 \frac{\mathrm{d}\kappa_1}{\kappa_1^{N_1+1}} \cdots \oint_0 \frac{\mathrm{d}\kappa_{g_\Sigma}}{\kappa_{g_\Sigma}^{N_{g_\Sigma}+1}} \, \Xi_X(\boldsymbol{\kappa};\hbar). \tag{3.34}$$

We can now use the argument first presented in [7]: the multi-contour integral can be written as an integral over μ_i, from $-\mathrm{i}\pi$ to $\mathrm{i}\pi$. Since, according to our conjecture (3.24), the generalized spectral determinant can be obtained by summing over all displacements of the μ_i parameters in integer steps of $2\pi\mathrm{i}$, we can trade the sum over the n_i by an integration along the whole imaginary axis, and we find

$$\begin{aligned} Z_X(\boldsymbol{N};\hbar) = \frac{1}{(2\pi\mathrm{i})^{g_\Sigma}} \int_{-\mathrm{i}\infty}^{\mathrm{i}\infty} \mathrm{d}\mu_1 \cdots \int_{-\mathrm{i}\infty}^{\mathrm{i}\infty} \mathrm{d}\mu_{g_\Sigma} \\ \times \exp\left\{ \mathsf{J}_X(\boldsymbol{\mu},\boldsymbol{\xi},\hbar) - \sum_{i=1}^{g_\Sigma} N_i \mu_i \right\}. \end{aligned} \tag{3.35}$$

As in [12], we want to evaluate the asymptotic expansion of the fermionic spectral traces in the 't Hooft limit (1.1). This can be done by evaluating the multi-integral in the saddle point approximation. To have a non-trivial limit as $\hbar \to \infty$, we have to consider the modified grand potential in the limit

$$\hbar \to \infty, \qquad \mu_i \to \infty, \qquad \frac{\mu_i}{\hbar} = \zeta_i \quad \text{fixed}, \quad i = 1, \ldots, g_\Sigma. \tag{3.36}$$

In this limit, the quantum mirror map becomes trivial, and we can replace t_i by its leading order term (3.2). We will also assume that the mass parameters $\boldsymbol{\xi}$ scale in such a way that

$$\frac{\log \xi_j}{\hbar}, \qquad j = 1, \ldots, r_\Sigma, \tag{3.37}$$

remain fixed in the 't Hooft limit (other scaling behaviors can be considered, as in [12]). In the study of the 't Hooft regime, we will denote $2\pi\mathbf{t}/\hbar$ simply

by $\mathbf{t}$, and $2\pi \log \xi_j/\hbar$ by $\log \xi_j$, to avoid unnecessary additional notation. From (3.2), we find that

$$t_i - \sum_{j=1}^{r_\Sigma} \alpha_{ij} \log \xi_j = 2\pi \sum_{j=1}^{g_\Sigma} C_{ij} \zeta_j, \qquad i = 1, \dots, g_\Sigma + r_\Sigma. \tag{3.38}$$

Then, in the limit (3.36), the modified grand potential has the genus expansion

$$\mathsf{J}_X^{\text{'t Hooft}}(\boldsymbol{\zeta}, \boldsymbol{\xi}, \hbar) = \sum_{g=0}^{\infty} \mathsf{J}_g^X(\boldsymbol{\zeta}, \boldsymbol{\xi})\, \hbar^{2-2g}, \tag{3.39}$$

where

$$\begin{aligned} \mathsf{J}_0^X(\boldsymbol{\zeta}, \boldsymbol{\xi}) &= \frac{1}{16\pi^4} \left(\widehat{F}_0(\mathbf{t}) + 4\pi^2 b_i^{\text{NS}} t_i + 16\pi^4 A_0(\boldsymbol{\xi}) \right), \\ \mathsf{J}_1^X(\boldsymbol{\zeta}, \boldsymbol{\xi}) &= A_1(\boldsymbol{\xi}) + \widehat{F}_1(\mathbf{t}), \\ \mathsf{J}_g^X(\boldsymbol{\zeta}, \boldsymbol{\xi}) &= A_g(\boldsymbol{\xi}) - C_g + (4\pi^2)^{2g-2} \widehat{F}_g(\mathbf{t}), \qquad g \geq 2. \end{aligned} \tag{3.40}$$

The arguments $\boldsymbol{\zeta}$ and $\boldsymbol{\xi}$ of the modified grand potential are related to the Kähler parameters $\mathbf{t}$ by (3.38). We have assumed that the function $A(\boldsymbol{\xi}, \hbar)$ has the expansion

$$A(\boldsymbol{\xi}, \hbar) = \sum_{g=0}^{\infty} A_g(\boldsymbol{\xi}) \hbar^{2-2g}. \tag{3.41}$$

In (3.40), as in (3.26), the $\widehat{F}_g(\mathbf{t})$ are the standard topological string free energies as a function of the Kähler parameters $\mathbf{t}$, after turning on the B-field. The saddle point of the integral (3.35) is given by

$$\lambda_i = \frac{C_{ji}}{8\pi^3} \left(\frac{\partial \widehat{F}_0}{\partial t_j} + 4\pi^2 b_j^{\text{NS}} \right), \qquad i = 1, \dots, g_\Sigma. \tag{3.42}$$

One then finds that the fermionic spectral traces have an expansion of the form (1.2). The leading function in this expansion is given by a Legendre transform,

$$\mathcal{F}_0(\boldsymbol{\lambda}) = \mathsf{J}_0^X(\boldsymbol{\zeta}, \boldsymbol{\xi}) - \boldsymbol{\lambda} \cdot \boldsymbol{\zeta}. \tag{3.43}$$

If we choose the Batyrev coordinates in such a way that the first g_Σ corresponds to true moduli and the remaining r_Σ correspond to mass parameters, we find

$$\frac{\partial \mathcal{F}_0}{\partial \lambda_i} = -\zeta_i = -\sum_{j=1}^{g_\Sigma} \frac{C_{ij}^{-1}}{2\pi} \left(t_j - \sum_{k=1}^{r_\Sigma} \alpha_{jk} \log \xi_k \right), \qquad i = 1, \dots, g_\Sigma, \tag{3.44}$$

where C^{-1} denotes the inverse of the truncated matrix (3.3). The higher genus corrections $\mathcal{F}_g(\boldsymbol{\lambda})$ in (1.2) can be computed systematically using the results of [60]. Indeed, the integral (3.35) implements a symplectic transformation from the large radius frame, to a particular frame which we will call the *maximal conifold frame*. As in [12], the 't Hooft coordinates λ_i are flat coordinates in this frame, and the maximal conifold locus is defined by

$$\lambda_i = 0, \qquad i = 1, \dots, g_\Sigma. \tag{3.45}$$

This locus has dimension r_Σ, the number of mass parameters of the toric CY. In case there are no mass parameters, as in the example of the resolved $\mathbb{C}^3/\mathbb{Z}_5$ orbifold considered in this paper, the maximal conifold locus is in fact a point, and we will refer to it sometimes as the maximal conifold point. It follows that the functions $\mathcal{F}_g(\boldsymbol{\lambda})$ appearing in (1.2) are the topological string genus g free energies in the maximal conifold frame. Note that (3.42) gives a prediction for the particular combination of periods which vanishes at the maximal conifold locus. As noted in [13], the coefficients of the constant trivial period are determined by the coefficients b_i^{NS}, i.e., the coefficients of the linear terms in the next-to-leading NS free energy. As far as we know, this connection has not been noticed before and is a direct consequence of our conjecture (3.24).

The main conclusion of this analysis is that, if (3.24) is correct, the fermionic spectral traces $Z_X(\boldsymbol{N}, \hbar)$ provide a non-perturbative definition of the genus expansion of the topological string (in the maximal conifold frame). This is of course the natural generalization of what was done in [12,13] in the case of genus one mirror curves. We will provide some detailed verifications of this statement in the case of the resolved $\mathbb{C}^3/\mathbb{Z}_5$ geometry, in the next section.

Finally, let us note that the fermionic spectral traces can be also computed in the so-called *M-theory limit*, in which $N_i \gg 1$ but $\hbar$ is fixed. In this limit, $Z_X(\boldsymbol{N}, \hbar)$ is given, at leading order, by a multivariable generalization of the Airy function, extending in this way the results found in the genus one case in [1]. In some cases, this generalization can be written as a product of conventional Airy functions. We will see a detailed example of this in Sect. 4.2.

4. Testing the Conjecture

In this section, we will perform a detailed test of the above conjectures in (arguably) the simplest toric geometry with a genus two mirror curve: the resolved $\mathbb{C}^3/\mathbb{Z}_5$ orbifold studied in the Example 2.1.

4.1. The Resolved $\mathbb{C}^3/\mathbb{Z}_5$ Orbifold

The toric description of the geometry is encoded in the charge vectors (2.27). After setting $x_1 = x_2 = x_4 = 1$, we have

$$z_1 = \frac{x_3}{x_0^3}, \qquad z_2 = \frac{x_0}{x_3^2}. \tag{4.1}$$

Another useful set of parameters for the moduli space are,

$$u = z_1 z_2^3 = x_3^{-5}, \quad v = z_1^2 z_2 = x_0^{-5}. \tag{4.2}$$

This geometry has been discussed in detail in [28,29], and it has a rich phase structure. The large radius point is, as usual,

$$z_1 = z_2 = 0. \tag{4.3}$$

In addition, there are two *half-orbifold points*. The first one is defined by

$$x_0 = 0, \quad u = 0, \tag{4.4}$$

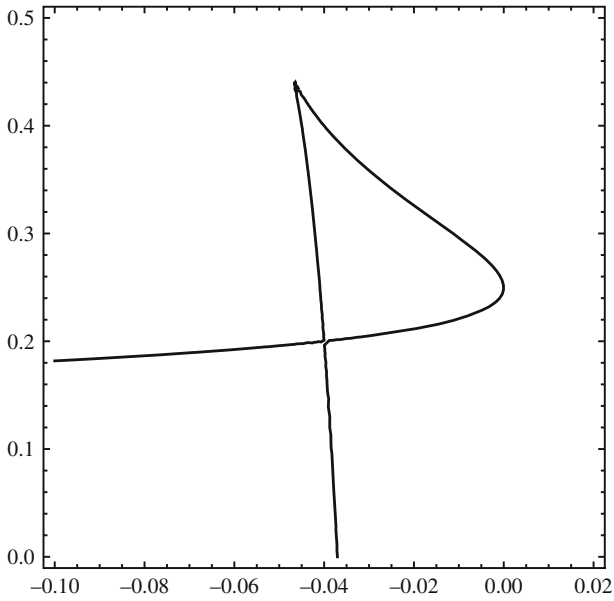

FIGURE 4. The conifold locus $\Delta(z_1, z_2) = 0$ in the (z_1, z_2) plane contains a point (4.8) where two components cross transversally

while the second one is defined by

$$x_3 = 0, \quad v = 0. \tag{4.5}$$

We note that these are the points which are suitable to study the operators $\mathsf{O}_{3,1}$ and $\mathsf{O}_{2,2}$, since in each case we are setting to zero the perturbation in (2.34). The corresponding geometries are the canonical bundles over $\mathbb{P}(1,3,1)$ and $\mathbb{P}(1,2,2)$, respectively. The (full) orbifold point is simply

$$x_0 = x_3 = 0. \tag{4.6}$$

As in the genus one case considered in [1], studying the topological string around this point will make it possible to calculate the expansion (2.57) of the generalized spectral determinant.

Another important region in the moduli space of the curve is the conifold locus, where the discriminant

$$\Delta(z_1, z_2) = 3125 z_1^2 z_2^3 + 500 z_1 z_2^2 + 16 z_2^2 - 225 z_1 z_2 - 8 z_2 + 27 z_1 + 1, \tag{4.7}$$

vanishes. The real part of this locus has various components, but there is a very special point at

$$z_1 = -\frac{1}{25}, \qquad z_2 = \frac{1}{5} \tag{4.8}$$

where two components of the locus cross transversally (see Fig. 4). As we will see, this is the maximal conifold point at which the 't Hooft parameters λ_1, λ_2

vanish. This point controls the 't Hooft limit of the spectral traces, at weak 't Hooft coupling.

The resolved $\mathbb{C}^3/\mathbb{Z}_5$ orbifold can be also realized as a perturbed local $\mathbb{P}^2$ geometry. This can be easily seen by considering the Eq. (2.30) and performing the transformation $x + y \to -x$. After reinstating x_4 in the equation, and setting $x_1 = x_2 = x_3 = 1$, we find that (2.30) reads,

$$\mathrm{e}^{x} + \mathrm{e}^{y} + \mathrm{e}^{-x-y} + x_4 \mathrm{e}^{2x} + x_0 = 0, \tag{4.9}$$

and we have

$$z_1 = x_0^{-3}, \qquad z_2 = x_4 x_0. \tag{4.10}$$

After Weyl quantization, we find the operator

$$\mathsf{O}_{1,1} + x_4 \mathrm{e}^{2\mathsf{x}}, \tag{4.11}$$

which is a perturbation of the operator $\mathsf{O}_{1,1}$ obtained by quantizing the mirror curve of local $\mathbb{P}^2$.

Let us now review some of the topological string amplitudes on this geometry. Near the large radius point there are two flat coordinates, t_1, t_2. They can be expressed in terms of the moduli z_1, z_2 by the mirror map,

$$\begin{aligned} t_1 &= -\Pi_{A_1}(z_1, z_2) = -\log(z_1) + \mathcal{O}(z_i), \\ t_2 &= -\Pi_{A_2}(z_1, z_2) = -\log(z_2) + \mathcal{O}(z_i), \end{aligned} \tag{4.12}$$

where the periods Π_{A_i}, Π_{B_i}, $i = 1, 2$ are given in (A.5). Using (2.28) and taking into account (3.2), we conclude that the matrix C_{ij} is given by

$$C = \begin{pmatrix} 3 & -1 \\ -1 & 2 \end{pmatrix}. \tag{4.13}$$

We will introduce, as usual, the exponentiated variables

$$Q_1 = \mathrm{e}^{-t_1}, \qquad Q_2 = \mathrm{e}^{-t_2}. \tag{4.14}$$

The large radius genus zero free energy is defined by the special geometry relations,

$$\frac{\partial F_0}{\partial t_1} = \frac{1}{10}\Pi_{B_1}, \qquad \frac{\partial F_0}{\partial t_2} = \frac{1}{10}\Pi_{B_2}, \tag{4.15}$$

which leads to (see for example [27])

$$F_0(t_1, t_2) = \frac{1}{15}t_1^3 + \frac{1}{10}t_1^2 t_2 + \frac{3}{10}t_1 t_2^2 + \frac{3}{10}t_2^3 + F_0^{\mathrm{inst}}(t_1, t_2), \tag{4.16}$$

where

$$F_0^{\mathrm{inst}}(t_1, t_2) = 3Q_1 - 2Q_2 - \frac{45}{8}Q_1^2 + 4Q_1 Q_2 - \frac{Q_2^2}{4} + \cdots \tag{4.17}$$

The genus one free energies (both standard and refined) have been obtained in [27]. The (standard) genus one free energy is given by

$$F_1(t_1, t_2) = -\frac{1}{12}\log\left(\Delta z_1^{38/5} z_2^{39/5}\right) - \frac{1}{2}\log\det(J_{ij}), \tag{4.18}$$

where

$$J_{ij} = \frac{\partial t_i}{\partial z_j} \tag{4.19}$$

is the Jacobian of the mirror map, and Δ is the discriminant (4.7). One finds, by explicit expansion,

$$F_1(t_1,t_2) = \frac{2t_1}{15} + \frac{3t_2}{20} + \frac{Q_1}{4} - \frac{Q_2}{6} - \frac{3Q_1^2}{8} + \frac{Q_1Q_2}{3} - \frac{Q_2^2}{12} + \cdots \tag{4.20}$$

Similarly, one finds the NS refined free energy,

$$F_1^{\mathrm{NS}}(t_1,t_2) = -\frac{1}{24}\log\left(\Delta z_1^{-2} z_2^{-3}\right), \tag{4.21}$$

which has the expansion

$$\begin{aligned} F_1^{\mathrm{NS}}(t_1,t_2) = &-\frac{t_1}{12} - \frac{t_2}{8} - \frac{7Q_1}{8} + \frac{Q_2}{6} \\ &+\frac{129Q_1^2}{16} - \frac{5Q_1Q_2}{6} + \frac{Q_2^2}{12} + \cdots . \end{aligned} \tag{4.22}$$

Higher genus free energies, as well as higher $F_n^{\mathrm{NS}}(t_1,t_2)$, have been determined in [27] up to order 3. We will, however, not use them in this paper.

4.2. The Generalized Spectral Determinant

The resolved $\mathbb{C}^3/\mathbb{Z}_5$ geometry involves two canonical operators, obtained by Weyl's quantization of (2.34). They read,

$$\begin{aligned} \mathsf{O}_1 &= \mathrm{e}^{\mathsf{x}} + \mathrm{e}^{\mathsf{y}} + \mathrm{e}^{-2\mathsf{x}-2\mathsf{y}} + x_3\mathrm{e}^{-\mathsf{x}-\mathsf{y}} = \mathsf{O}_{2,2} + x_3\mathrm{e}^{-\mathsf{x}-\mathsf{y}}, \\ \mathsf{O}_2 &= \mathrm{e}^{\mathsf{x}} + \mathrm{e}^{\mathsf{y}} + \mathrm{e}^{-3\mathsf{x}-\mathsf{y}} + x_0\mathrm{e}^{-\mathsf{x}} = \mathsf{O}_{3,1} + x_0\mathrm{e}^{-\mathsf{x}}. \end{aligned} \tag{4.23}$$

As we have seen in Sect. (2.3), the generalized spectral determinant can be expressed in many ways. A particularly useful representation in this geometry comes from (2.75), and we find

$$\begin{aligned} \Xi(x_0,x_3;\hbar) &= \det\left(1 + x_0\left(\mathsf{O}_{2,2} + x_3\mathsf{P}_{12}\right)^{-1}\right)\det\left(1 + x_3\mathsf{O}_{3,1}^{-1}\right) \\ &= \det\left(1 + x_3\left(\mathsf{O}_{3,1} + x_0\mathsf{P}_{21}\right)^{-1}\right)\det\left(1 + x_0\mathsf{O}_{2,2}^{-1}\right). \end{aligned} \tag{4.24}$$

In particular, we have

$$\begin{aligned} \det\left(1 + x_0\left(\mathsf{O}_{2,2} + x_3\mathsf{P}_{12}\right)^{-1}\right) &= \frac{\Xi(x_0,x_3;\hbar)}{\Xi(0,x_3;\hbar)}, \\ \det\left(1 + x_3\left(\mathsf{O}_{3,1} + x_0\mathsf{P}_{21}\right)^{-1}\right) &= \frac{\Xi(x_0,x_3;\hbar)}{\Xi(x_0,0;\hbar)}. \end{aligned} \tag{4.25}$$

The defining formula for the generalized spectral determinant is (2.54). For convenience, we will choose as our reference operator $\mathsf{O}_{3,1}$ (i.e., we will choose $j = 2$ in (2.54)). The relevant operators are then,

$$\mathsf{A}_{21} = \rho_{3,1}\mathsf{P}_{21}, \qquad \mathsf{A}_{22} = \rho_{3,1}, \tag{4.26}$$

and we recall that

$$\mathsf{P}_{21} = \mathrm{e}^{-\mathsf{x}}, \tag{4.27}$$

where x is the quantum Heisenberg operator appearing in $\mathsf{O}_{3,1}$. It is known from [11] that $\rho_{3,1}$ is of trace class, and it can be easily checked that A_{21} is of trace class as well.

We are now ready to write down the total grand potential, as it follows from our conjecture (3.24). The parameters entering the operators are written in terms of chemical potentials as,

$$x_0 = \kappa_1 = \mathrm{e}^{\mu_1}, \qquad x_3 = \kappa_2 = \mathrm{e}^{\mu_2}, \tag{4.28}$$

and they are related to the complex moduli of the geometry by

$$\log z_1 = -3\mu_1 + \mu_2, \qquad \log z_2 = \mu_1 - 2\mu_2, \tag{4.29}$$

as it follows from (3.2). The first thing we must know is the value of the appropriate B-field in (3.18). Since this geometry can be regarded as a perturbation of the local $\mathbb{P}^2$ geometry when $z_2 = 0$, a natural guess is that

$$\mathbf{B} = (1, 0). \tag{4.30}$$

It can be checked that, for this choice, (3.19) is satisfied.[2] The insertion of this B-field in the worldsheet instanton piece is equivalent to changing the sign of Q_1 in the expansions at large radius (but not in the log terms). For example, for the very first terms, one finds,

$$\begin{aligned} \mathsf{J}^{\mathrm{WS}}(\mu_1, \mu_2; \hbar) = &- \sum_{v=1}^{\infty} \frac{1}{v} \left(2 \sin \frac{2\pi^2 v}{\hbar} \right)^{-2} \\ &\times \left(3\mathrm{e}^{-2\pi v t_1/\hbar} + 2\mathrm{e}^{-2\pi v t_2/\hbar} \right) + \cdots , \end{aligned} \tag{4.31}$$

and the sign in the first exponential (involving t_1) is the opposite one to what we had in (4.17).

The function $\mathsf{J}^{\mathrm{WKB}}(\mu_1, \mu_2; \hbar)$ can be computed in many different ways. The leading order terms at large μ_i can be read from (4.16), (4.20) and (4.22). The semiclassical limit (3.17) can be checked as in [6], by calculating semiclassical traces. This calculation is easy to do either when $x_3 = 0$, or when $x_0 = 0$. In these cases, the relevant operators are simply $\mathsf{O}_{2,2}$, $\mathsf{O}_{3,1}$, respectively, and the corresponding semiclassical grand potential is easy to calculate (see also [61]). The classical spectral traces of these operators are

$$\begin{aligned} Z_\ell^{(0)}(\mathsf{O}_{2,2}) &= \int \frac{\mathrm{d}x\mathrm{d}y}{2\pi} \frac{1}{\left(\mathrm{e}^x + \mathrm{e}^y + \mathrm{e}^{-2x-2y}\right)^\ell} \\ &= \frac{1}{10\pi} \frac{\Gamma(\ell/5)\,\Gamma(2\ell/5)^2}{\Gamma(\ell)}, \\ Z_\ell^{(0)}(\mathsf{O}_{3,1}) &= \int \frac{\mathrm{d}x\mathrm{d}y}{2\pi} \frac{1}{\left(\mathrm{e}^x + \mathrm{e}^y + \mathrm{e}^{-3x-y}\right)^\ell} \\ &= \frac{1}{10\pi} \frac{\Gamma(\ell/5)^2\,\Gamma(3\ell/5)}{\Gamma(\ell)}. \end{aligned} \tag{4.32}$$

[2] We would like to thank Albrecht Klemm for verifying explicitly that this is indeed the case for the refined BPS invariants of this geometry calculated in [27].

We then find,

$$\mathsf{J}_0(\mu_1,0) = -\sum_{\ell=1}^{\infty} \frac{(-\kappa_1)^\ell}{\ell} Z_\ell^{(0)}\left(\mathsf{O}_{2,2}\right),$$
$$\mathsf{J}_0(0,\mu_2) = -\sum_{\ell=1}^{\infty} \frac{(-\kappa_2)^\ell}{\ell} Z_\ell^{(0)}\left(\mathsf{O}_{3,1}\right). \tag{4.33}$$

From the point of view of the geometry, these are expansions near the orbifold point. It is easy to verify, using the explicit formulae in Sect. A.2 of the Appendix, that these expansions are indeed reproduced by the r.h.s. of (3.17). Finally, the quantum mirror map entering in the expression (3.22) can be computed systematically, as shown in Appendix A.4.

As we explained above, in the maximally supersymmetric case $\hbar = 2\pi$, the spectral determinant can be written down explicitly. The generalized theta function becomes in this case a standard Riemann theta function. Indeed, it can be easily checked that

$$\Theta(\boldsymbol{\mu}; 2\pi) = \sum_{n_1,n_2\in\mathbb{Z}} \exp\times\Big[\mathrm{i}\pi\left(n_1^2\tau_{11} + 2n_1n_2\tau_{12} + n_2^2\tau_{22}\right) + 2\pi\mathrm{i}\left(n_1\upsilon_1 + n_2\upsilon_2\right) - \mathrm{i}\pi\left(n_1 + \frac{8}{3}n_2\right)\Big], \tag{4.34}$$

where the vector $\boldsymbol{\upsilon}$ is given in (3.30) (since we are considering a fixed CY example, we have removed the subscript X). Let us recall that the Riemann theta function with characteristics $\boldsymbol{\alpha}$, $\boldsymbol{\beta}$ is defined by

$$\vartheta\begin{bmatrix}\boldsymbol{\alpha}\\ \boldsymbol{\beta}\end{bmatrix}(\boldsymbol{z},\tau) = \sum_{\boldsymbol{n}\in\mathbb{Z}^2} \exp\left[\mathrm{i}\pi\ {}^t(\boldsymbol{n}+\boldsymbol{\alpha})\tau(\boldsymbol{n}+\boldsymbol{\alpha}) + 2\pi\mathrm{i}(\boldsymbol{z}+\boldsymbol{\beta})\cdot(\boldsymbol{n}+\boldsymbol{\alpha})\right]. \tag{4.35}$$

It follows that the generalized spectral determinant, for the maximally supersymmetric case, can be written as

$$\Xi(\boldsymbol{\mu}; 2\pi) = \exp\left(\mathsf{J}(\boldsymbol{\mu}; 2\pi)\right)\vartheta\begin{bmatrix}\mathbf{0}\\ \boldsymbol{\beta}\end{bmatrix}(\boldsymbol{\upsilon},\tau). \tag{4.36}$$

where

$$\boldsymbol{\beta} = -\left(\frac{1}{2},\frac{4}{3}\right) \tag{4.37}$$

and $\mathsf{J}(\boldsymbol{\mu}; 2\pi)$ is given by the specialization of (3.26) to the resolved $\mathbb{C}^3/\mathbb{Z}_5$ orbifold. It is also easy to check from the results in the Appendix A.4 that, for $\hbar = 2\pi$, the quantum mirror map becomes the classical mirror map, together with a change of sign $z_1 \to -z_1$ in the polynomial part.

The expression (4.36) embodies our conjecture for the case at hand. We can now test our conjecture by verifying that this formula indeed gives the right spectral properties and quantities (in the maximally supersymmetric case). In the rest of this section, we will check the predictions for the spectral traces.

The fermionic spectral traces $Z(N_1, N_2; \hbar)$ can be read off from the expansion of the spectral determinant around $\kappa_1 = \kappa_2 = 0$, which in our case corresponds to $x_0 = x_3 = 0$. This is the orbifold point. In the maximally supersymmetric case, this can be done by performing an analytic continuation of the various quantities involved in (4.34) to the orbifold point. As in the case of local $\mathbb{P}^2$ analyzed in [1], it is convenient to change the sign of x_3 and perform the expansion of a closely related theta function. Note that this leads to a change of sign $z_1 \to -z_1$. This has the effect of restoring the conventional sign of the standard topological string amplitudes (which we had to change, due to the B-field (4.30)), but also changes the structure of the theta function, due to the shifts in the logarithms. After carefully keeping track of all these changes, we find,

$$\Xi(x_0, -x_3; 2\pi) = \mathrm{e}^{\mathsf{J}(x_0, x_3; 2\pi)} \mathrm{e}^{\mathrm{i}\pi\vartheta} \begin{bmatrix} \boldsymbol{\alpha} \\ \boldsymbol{\beta} \end{bmatrix} (\boldsymbol{\upsilon}, \tau - S)\,, \tag{4.38}$$

where

$$S = \begin{pmatrix} 1/2 & 1/2 \\ 1/2 & 0 \end{pmatrix}, \quad \boldsymbol{\alpha} = \left(0, \frac{1}{2}\right), \quad \boldsymbol{\beta} = -\left(\frac{3}{8}, \frac{4}{3}\right), \tag{4.39}$$

and the quantities $\mathsf{J}(x_0, x_3; 2\pi)$, τ and $\boldsymbol{\upsilon}$ are given by (3.26), (3.28) and (3.30) but they involve now the analytic continuation to the orbifold point of the *standard* genus zero and one free energies. After implementing this formula, one finds the expansion

$$\Xi(x_0, x_3; 2\pi) = 1 + Z(1, 0; 2\pi) x_0 + Z(0, 1; 2\pi) x_3 + Z(1, 1; 2\pi) x_0 x_3 + \cdots \tag{4.40}$$

The coefficients of this expansion involve derivatives of the Riemann theta function of genus two, but they can be evaluated numerically with high precision. We find,

$$\begin{aligned} Z(1, 0; 2\pi) &= 0.0552786404500042\ldots, \\ Z(0, 1; 2\pi) &= 0.0894427190999916\ldots, \\ Z(1, 1; 2\pi) &= 0.0030770561988687\ldots \end{aligned} \tag{4.41}$$

As we explained in Sect. 2.3, these coefficients are defined as (generalized) fermionic spectral traces of the operators (4.26). One has, for example,

$$\begin{aligned} Z(1, 0; 2\pi) &= \mathrm{Tr}\,(\rho_{3,1} \mathsf{P}_{21}) = \mathrm{Tr}\rho_{2,2}, \\ Z(0, 1; 2\pi) &= \mathrm{Tr}\rho_{3,1}, \\ Z(1, 1; 2\pi) &= \mathrm{Tr}\rho_{2,2}\,\mathrm{Tr}\rho_{3,1} - \mathrm{Tr}(\rho_{3,1}\mathsf{P}_{21}\rho_{3,1}). \end{aligned} \tag{4.42}$$

In [11], the integral kernels of the operators $\rho_{m,n}$ were obtained in closed form, in terms of the quantum dilogarithm. Therefore, the traces (4.42) can be computed explicitly. Since these results will be also used in the analysis near the maximal conifold point, let us briefly summarize them. Let us denote by $\Phi_{\mathsf{b}}(x)$ Faddeev's quantum dilogarithm [62,64] (we follow the notations in [11]). We define as well the functions (see also [68])

$$\Psi_{a,c}(x) = \frac{\mathrm{e}^{2\pi a x}}{\Phi_{\mathsf{b}}(x - \mathrm{i}(a + c))}. \tag{4.43}$$

Let q, p be operators satisfying the normalized Heisenberg commutation relation

$$[\mathsf{p}, \mathsf{q}] = (2\pi \mathsf{i})^{-1}. \tag{4.44}$$

They are related to the Heisenberg operators x, y appearing in $\mathsf{O}_{m,n}$ by the following linear canonical transformation:

$$\mathsf{x} \equiv 2\pi \mathsf{b} \frac{(n+1)\mathsf{p} + n\mathsf{q}}{m+n+1}, \quad \mathsf{y} \equiv -2\pi \mathsf{b} \frac{m\mathsf{p} + (m+1)\mathsf{q}}{m+n+1}, \tag{4.45}$$

so that $\hbar$ is related to b by

$$\hbar = \frac{2\pi \mathsf{b}^2}{m+n+1}. \tag{4.46}$$

Then, in the momentum representation associated with p, the operator $\rho_{m,n}$ has the integral kernel,

$$\rho_{m,n}(p, p') = \frac{\overline{\Psi_{a,c}(p)}\, \Psi_{a,c}(p')}{2\mathsf{b} \cosh\left(\pi \frac{p - p' + \mathsf{i}(a+c-nc)}{\mathsf{b}}\right)}, \tag{4.47}$$

where a, c are given by

$$a = \frac{m\mathsf{b}}{2(m+n+1)}, \qquad c = \frac{\mathsf{b}}{2(m+n+1)}. \tag{4.48}$$

Using these results, we can easily compute the kernel of A_{21}, and one finds

$$\langle p | \rho_{3,1} \mathsf{P}_{21} | p' \rangle = \mathrm{e}^{-\frac{4\pi \mathsf{b} p'}{5}} \mathrm{e}^{-\frac{2\pi \mathsf{b}^2 \mathsf{i}}{25}} \rho_{3,1}\left(p, p' + \frac{\mathsf{i}\mathsf{b}}{5}\right). \tag{4.49}$$

Therefore, we find the following integral representation

$$\mathrm{Tr}(\rho_{3,1} \mathsf{P}_{21} \rho_{3,1}) = \mathrm{e}^{-\frac{2\pi \mathsf{b}^2 \mathsf{i}}{25}} \int \mathrm{e}^{-\frac{4\pi \mathsf{b} p'}{5}} \rho_{3,1}\left(p, p' + \frac{\mathsf{i}\mathsf{b}}{5}\right) \rho_{3,1}(p', p)\, \mathrm{d}p\, \mathrm{d}p'. \tag{4.50}$$

In the maximally supersymmetric case, $\hbar = 2\pi$, the spectral theory of these operators also simplifies, as noted already in [10], and one can use the results of [63] to show that the integral kernels above become elementary functions. The trace of $\rho_{m,1}$ was computed in [11] for any m and $\hbar = 2\pi$, and one finds

$$\mathrm{Tr}\, \rho_{3,1} = \frac{1}{5\sqrt{5}}. \tag{4.51}$$

A similar computation shows that

$$\mathrm{Tr}\, \rho_{2,2} = \frac{1}{50}\left(5 - \sqrt{5}\right). \tag{4.52}$$

These agree *precisely* with the predictions (4.41) of the spectral determinant (4.36). A numerical calculation of the double-integral (4.50) makes it also possible to verify the prediction in (4.41) for $Z(1, 1; 2\pi)$.

We should note that, although we evaluated the expansion (4.40) numerically, its coefficients can be computed analytically in terms of derivatives of the Riemann–Siegel theta function. For example, one finds

$$Z(1,0;2\pi)=\frac{2^{9/5}\mathrm{i}\sqrt{\frac{\pi}{5}}\Gamma\left(\frac{9}{10}\right)}{\Gamma\left(\frac{1}{5}\right)^2}\left(\Theta_{11}(\boldsymbol{v}_0,\tau_0)+\frac{1}{2}\Theta_{12}(\boldsymbol{v}_0,\tau_0)-\Theta_{22}(\boldsymbol{v}_0,\tau_0)\right), \tag{4.53}$$

where

$$\Theta_{ij}(\boldsymbol{v}_0,\tau_0)=\frac{\partial_{\tau_{ij}}\vartheta\begin{bmatrix}\boldsymbol{\alpha}\\ \boldsymbol{\beta}\end{bmatrix}(\boldsymbol{v}_0,\tau_0)}{\vartheta\begin{bmatrix}\boldsymbol{\alpha}\\ \boldsymbol{\beta}\end{bmatrix}(\boldsymbol{v}_0,\tau_0)},\quad \boldsymbol{\alpha}=\left(0,\frac{1}{2}\right),\quad \boldsymbol{\beta}=\left(\frac{3}{8},\frac{4}{3}\right), \tag{4.54}$$

and

$$\begin{aligned}\boldsymbol{v}_0&=\left(-\frac{11}{40},-\frac{1}{30}\right),\\ \tau_0&=\begin{pmatrix}-\frac{1}{2}+\frac{1}{2}\mathrm{i}\sqrt{\frac{1}{5}\left(5+2\sqrt{5}\right)} & -\frac{1}{2}+\mathrm{i}\sqrt{\frac{1}{4}-\frac{1}{2\sqrt{5}}}\\ -\frac{1}{2}+\mathrm{i}\sqrt{\frac{1}{4}-\frac{1}{2\sqrt{5}}} & \mathrm{i}\sqrt{\frac{1}{10}\left(5+\sqrt{5}\right)}\end{pmatrix}.\end{aligned} \tag{4.55}$$

Moreover, by requiring that $Z(0,0;2\pi)=1$, we find the following identity:

$$\vartheta\begin{bmatrix}\boldsymbol{\alpha}\\ \boldsymbol{\beta}\end{bmatrix}(\boldsymbol{v}_0,\tau_0)=-\frac{5^{7/40}\Gamma\left(\frac{1}{5}\right)^{3/2}}{2^{2/5}\left(5+\sqrt{5}\right)^{3/5}\pi\sqrt{\Gamma\left(\frac{3}{5}\right)}}, \tag{4.56}$$

which we checked numerically with high precision. The fact that (4.53) agrees with (4.52) is another manifestation of the highly non-trivial content of our conjecture (3.24).

There is yet another method to evaluate the spectral traces, which can be also applied away from the maximally supersymmetric case. This method, which goes back to [7], is based on the integral formula (3.35), and in using directly the large radius expansion of the modified grand potential. In the genus one case, where there is one single integration, this leads to an expression for the fermionic spectral traces given by an infinite sum of Airy functions, in which each term is exponentially suppressed with respect to the preceding one. It turns out that this method can be generalized to the resolved $\mathbb{C}^3/\mathbb{Z}_5$, as follows. The modified grand potential is given by

$$\mathsf{J}(\mu_1,\mu_2;\hbar)=\mathsf{J}^{(\mathrm{p})}(\mu_1,\mu_2;\hbar)+\mathsf{J}^{(\mathrm{np})}(\mu_1,\mu_2;\hbar). \tag{4.57}$$

Here, the perturbative part is the cubic polynomial in the μ_is,

$$\begin{aligned}\mathsf{J}^{(\mathrm{p})}(\mu_1,\mu_2;\hbar)=&\frac{1}{\pi\hbar}\left(\frac{3\mu_1^3}{4}-\frac{3\mu_2\mu_1^2}{4}+\frac{\mu_2^2\mu_1}{4}+\frac{2\mu_2^3}{3}\right)\\ &+\frac{1}{2}\left(\frac{\pi}{\hbar}-\frac{\hbar}{8\pi}\right)\mu_1+\frac{1}{3}\left(\frac{\pi}{\hbar}-\frac{\hbar}{4\pi}\right)\mu_2+A(\hbar),\end{aligned} \tag{4.58}$$

while the non-perturbative part $\mathsf{J}^{(\mathrm{np})}(\mu_1,\mu_2;\hbar)$ contains the exponentially small corrections appearing in the expression (3.22), and it is a power series in z_1, z_2. We recall that the complex moduli $z_{1,2}$ are related to the parameters $\mu_{1,2}$ by (4.29). We can now make a change of variables such that the cubic polynomial appearing in (4.58) does not contain mixed terms,

$$\mu_1 = \nu_1 + \frac{\nu_2}{3}, \qquad \mu_2 = \nu_2. \tag{4.59}$$

We find,

$$\mathsf{J}^{(\mathrm{p})}(\nu_1,\nu_2;\hbar) = \sum_{i=1}^{2}\left(\frac{C_i(\hbar)}{3}\nu_i^3 + B_i(\hbar)\nu_i\right) + A(\hbar), \tag{4.60}$$

where

$$C_1(\hbar) = \frac{9}{4\pi\hbar}, \qquad C_2(\hbar) = \frac{25}{12\pi\hbar}, \tag{4.61}$$

and

$$\begin{aligned} B_1(\hbar) &= \frac{1}{2}\left(\frac{\pi}{\hbar} - \frac{\hbar}{8\pi}\right), \\ B_2(\hbar) &= \frac{1}{2}\left(\frac{\pi}{\hbar} - \frac{5\hbar}{24\pi}\right). \end{aligned} \tag{4.62}$$

It follows from (3.35) that the fermionic spectral traces are given, at leading order, by

$$Z(N_1,N_2;\hbar) \approx Z^{(\mathrm{p})}(N_1,N_2;\hbar), \tag{4.63}$$

where

$$Z^{(\mathrm{p})}(N_1,N_2;\hbar) = \mathrm{e}^{A(\hbar)}\prod_{i=1}^{2}\left(C_i(\hbar)\right)^{-1/3}\mathrm{Ai}\left[\left(C_i(\hbar)\right)^{-1/3}\left(M_i - B_i(\hbar)\right)\right], \tag{4.64}$$

and the M_i are defined by the condition,

$$\boldsymbol{\mu}\cdot\boldsymbol{N} = \boldsymbol{\nu}\cdot\boldsymbol{M}, \tag{4.65}$$

so that, in this case,

$$M_1 = N_1, \qquad M_2 = \frac{N_1}{3} + N_2. \tag{4.66}$$

It is also clear how to incorporate the corrections due to $\mathsf{J}^{(\mathrm{np})}(\mu_1,\mu_2;\hbar)$. We can write,

$$\mathrm{e}^{\mathsf{J}^{(\mathrm{np})}(\mu_1,\mu_2;\hbar)} = \sum_{i,j\geq 0} P_{i,j}(\mu_1,\mu_2;\hbar) z_1^i z_2^j, \tag{4.67}$$

where the $P_{i,j}(\mu_1,\mu_2;\hbar)$ are polynomials in μ_1,μ_2, and $P_{0,0} = 1$. Then, a simple computation shows that

$$\begin{aligned} Z(N_1,N_2;\hbar) = \sum_{i,j\geq 0} & P_{i,j}\left(-\partial_{N_1},-\partial_{N_2};\hbar\right) Z^{(\mathrm{p})} \\ & \times\left(N_1+3i-j, N_2-i+2j;\hbar\right). \end{aligned} \tag{4.68}$$

The leading term in this expression is of course given by (4.64), while the remaining series gives, for N_i large, exponentially small corrections. As in the case of genus one mirror curves, this expansion seems to converge rapidly, and we have verified that, for $\hbar = 2\pi$, it reproduces the spectral traces computed above. In addition, we found the following educated guess for the value of $A(2\pi)$,

$$A(2\pi) = \frac{1}{10} \log\left(\frac{25}{2}\left(5+\sqrt{5}\right)\right) - \frac{3\zeta(3)}{5\pi^2}. \tag{4.69}$$

The formula (4.64) generalizes the results involving Airy functions found in Chern–Simons matter theories [6,65] and in the case of topological strings on local del Pezzo surfaces [1]. It has been recently shown in [66] that the Airy behavior of the topological string partition function is a universal feature. In [66], this behavior (involving a single Airy function) was obtained by considering a one-dimensional slice of the moduli space. It would be interesting to see if the argument of [66] can be used to derive (4.64). Note that, if g_Σ is large enough, we cannot put to zero all the crossing terms in the cubic polynomial appearing in $\mathsf{J}^{(\mathrm{p})}(\boldsymbol{\mu};\hbar)$, and the leading behavior of the fermionic spectral traces will be given by a generalization of the Airy function which does not reduce to a product of elementary Airy functions.

4.3. Quantization Conditions

One of the most important results of [1] is that, in the case of mirror curves of genus one, the quantization condition for the spectrum of the corresponding operator can be read from the vanishing of the (deformed) theta function entering in the spectral determinant. As it was already pointed out in [1], there is a natural generalization of this conjecture to the higher genus case, by considering the vanishing of the higher genus, deformed theta function in (3.25). However, the higher genus case is richer (and slightly more complicated) due to the fact that there are many operators O_i, $i = 1, \ldots, g_\Sigma$, which one can associate to the same geometry. Let us explain this in some more detail.

The vanishing of the generalized spectral determinant gives a *global* quantization condition, which defines a discrete family of codimension one submanifolds in moduli space. In many cases, a given point in the vanishing locus solves the spectral problem for different (related) operators. For example, the resolved $\mathbb{C}^3/\mathbb{Z}_5$ orbifold leads to two different operators (4.23). A point (x_0, x_3) in the vanishing locus of the spectral determinant, with $x_0 < 0$ and $x_3 < 0$, can be interpreted in two ways: either as an eigenvalue $-x_0$ of the operator O_1, which depends on x_3, or an eigenvalue $-x_3$ for the operator O_2, which depends on x_0. This follows from the discussion around (2.79). However, if the point in the vanishing locus occurs at $x_0 = 0$, it cannot be interpreted in terms of O_1, since this operator is positive definite and all its eigenvalues are strictly positive.

In this section, we will obtain the quantization condition for $\mathbb{C}^3/\mathbb{Z}_5$, in the maximally supersymmetric case, and verify explicitly that it solves many different spectral problems. In particular, we will be able to write exact quantization conditions for the unperturbed operators $\mathsf{O}_{3,1}$ and $\mathsf{O}_{2,2}$. To have a

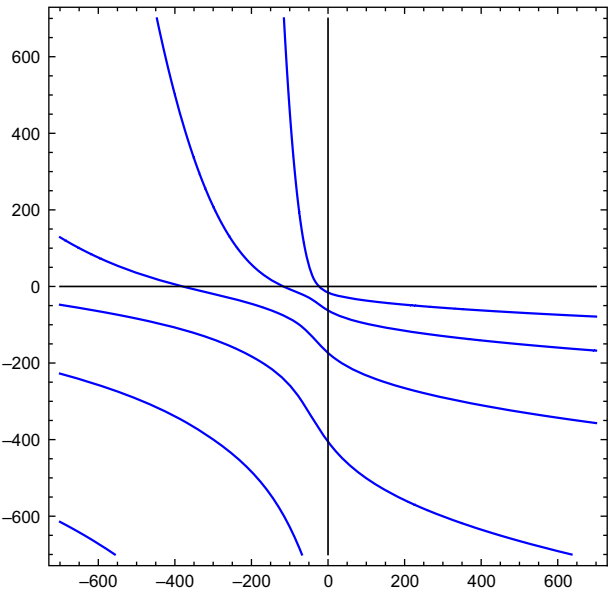

FIGURE 5. The *curves* represent the locus in the (x_0, x_3) plane in which the generalized spectral determinant (4.36) vanishes. They can be labeled by the quantum number $n = 0, 1, \ldots$ appearing in the generalized Bohr–Sommerfeld quantization condition. The uppermost curve corresponds to $n = 0$

first view of the vanishing locus of the generalized spectral determinant (4.36) in the moduli space parametrized by (x_0, x_3), we can simply plot it using the expansion (4.40) (we assume that x_0 and x_3 are real). The result is shown in Fig. 5. It consists of a discrete family of curves, and each curve crosses both the negative x_3 and x_0 axis. Note that there are no solutions in which both x_0 and x_3 are positive. The vanishing locus obtained in this way has all the expected properties: the intersection with the axis $x_3 = 0$ and $x_0 = 0$ gives the spectrum of the operators $\rho_{2,2}$ and $\rho_{3,1}$. The discrete family of curves correspond to the quantum numbers $n = 0, 1, \ldots$ of the generalized Bohr–Sommerfeld quantization condition.

As a first test that this vanishing locus produces the actual spectrum, we can compute the ground-state energy for the operators $\rho_{2,2}$ and $\rho_{1,1}$, using the diagonalization method of [67], and compare it with the zeros of the spectral determinant $\Xi(x_0, 0; 2\pi)$ and $\Xi(0, x_3; 2\pi)$, as we keep more and more terms in their polynomial expansion. We recall that, if these functions vanish at $(x_0, 0)$ and $(0, x_3)$, respectively, the energies are given by

$$E = \log(-x_0), \qquad E = \log(-x_3). \tag{4.70}$$

As we see in Tables 1 and 2, the answer obtained from the spectral determinant converges rapidly to the correct value.

TABLE 1. The ground-state energy E_0 for the operator $\rho_{2,2}$, as obtained from the vanishing locus of the spectral determinant $\Xi(x_0, 0; 2\pi)$

Order	E_0
1	2.8953686937107540094
5	3.1640650172200080194
8	3.1640650781321192069
10	3.1640650781321190565
Numerical value	3.1640650781321190565

This is a power series around $x_0 = 0$, and to obtain the energy we truncate it at a given order in x_0. As we keep more and more terms in the series, we quickly approach the ground-state energy obtained by numerical methods

TABLE 2. The ground-state energy E_0 for the operator $\rho_{3,1}$, as obtained from the vanishing locus of the spectral determinant $\Xi(0, x_3; 2\pi)$

Order	E_0
1	2.4141568686511505619
5	2.7700028996745256210
8	2.7700040488404954468
10	2.7700040488404460337
Numerical value	2.7700040488404460337

We follow the same procedure as in Table 1

The expansion (4.40) around the orbifold point is very convenient for small energies, but it does not make contact with the WKB expansion for the operators $\rho_{2,2}$ and $\rho_{3,1}$. We can, however, obtain alternative formulations of the exact quantization condition for these operators using expansions appropriate for the half-orbifold points. Let us first consider the operator $\rho_{2,2}$. In principle, the zeroes of the spectral determinant occur at negative values of x_0 and x_3, but it is convenient to change their signs so that they occur along the positive real axis. In the case of $\rho_{2,2}$, we change the sign of x_0, which involves changing the sign of both z_1 and z_2. The quantization condition is given by the vanishing of the theta function

$$\Theta_{2,2}(E) = \vartheta \begin{bmatrix} \boldsymbol{\alpha} \\ \boldsymbol{\beta} \end{bmatrix} (\boldsymbol{\upsilon}, \tau - S)\,, \tag{4.71}$$

where

$$\boldsymbol{\alpha} = \left(\frac{1}{2}, 0\right), \quad \boldsymbol{\beta} = \left(-\frac{3}{8}, \frac{7}{24}\right), \qquad S = \begin{pmatrix} 1/2 & 1/2 \\ 1/2 & 1/2 \end{pmatrix}. \tag{4.72}$$

In this theta function, $\boldsymbol{\upsilon}$, τ are computed using the analytic continuations (A.29), we set $x_3 = 0$, and $E = -\log(Y)$.

In the case of $\rho_{3,1}$, we change the sign of x_3, which involves changing the sign of z_1. We already did this in the calculation near the full orbifold point,

and we find that the quantization condition is given by the vanishing of the theta function,

$$\Theta_{3,1}(E) = \vartheta \begin{bmatrix} \boldsymbol{\alpha} \\ \boldsymbol{\beta} \end{bmatrix} (\boldsymbol{\upsilon}, \tau - S)\,, \tag{4.73}$$

where $\boldsymbol{\alpha}$, $\boldsymbol{\beta}$ and S are given in (4.39), $\boldsymbol{\upsilon}$, τ are computed using the analytic continuations (A.20), (A.24), we set $x_0 = 0$, and $E = -\log(X)$.

It is interesting to see in some detail how the above quantization conditions agree, in the limit of large energies, with the semiclassical result. Let us consider, for example, the operator $\rho_{3,1}$. The semiclassical quantization condition can be obtained using for example Fermi gas technology. The grand potential for the operator $\rho_{3,1}$ at large μ is given by

$$\mathcal{J}(\mu, \hbar) \approx \frac{25}{36\pi\hbar}\mu^3 + \left(\frac{\pi}{2\hbar} - \frac{5\hbar}{48\pi}\right)\mu, \qquad \mu \gg 1. \tag{4.74}$$

This follows from formulae (5.8) and (B.2) of [61]. Using the general results of [6], one finds that the quantization condition at large E is given by

$$\mathrm{vol}(E) = 2\pi\hbar\left(n + \frac{1}{2}\right), \tag{4.75}$$

where

$$\mathrm{vol}(E) \approx \frac{25}{6}E^2 - \frac{7\pi^2}{18} - \frac{5\hbar^2}{24\pi}, \qquad E \gg 1. \tag{4.76}$$

This includes the first-order correction in $\hbar^2$. How can this be obtained from $\Theta_{3,1}(E)$? First, we have to understand the structure of the various functions involved in the higher genus theta function. One finds, from the formulae in Appendix A.2,

$$\begin{aligned} \tau_{11} &= \frac{\mathrm{i}\sqrt{3}}{2} + \mathcal{O}(X^{10/3}), \\ \tau_{12} &= -\frac{\mathrm{i}}{2\sqrt{3}} + \mathcal{O}(X^{5/3}), \\ \tau_{22} &= -\frac{25\mathrm{i}}{6\pi}\log(X) + \frac{\mathrm{i}}{6\sqrt{3}} + \mathcal{O}(X^{5/3}), \end{aligned} \tag{4.77}$$

as well as

$$\begin{aligned} \upsilon_1 &= \frac{5}{24} + \mathcal{O}(X^{5/3}), \\ \upsilon_2 &= \frac{25\log^2(X)}{24\pi^2} - \frac{1}{36} + \mathcal{O}(X^{5/3}). \end{aligned} \tag{4.78}$$

The terms involving positive powers of X are exponentially small corrections. We would like now to obtain the vanishing condition for $\Theta_{3,1}(E)$ at leading order, neglecting these small corrections. It is easy to see, from the above behaviors, that the leading contribution comes from the terms with $n_2 = 0, -1$ in the theta function. More precisely, one finds the vanishing condition

$$\cos\left(\pi\left(-\upsilon_2 + 1/3\right) + \phi\right) = 0. \tag{4.79}$$

Here, ϕ is the argument of the (genus one) Jacobi theta function

$$\vartheta \begin{bmatrix} 0 \\ 0 \end{bmatrix} \left(\frac{5}{12} - \frac{\mathrm{i}}{4\sqrt{3}}, \frac{1}{2} + \frac{\mathrm{i}\sqrt{3}}{2} \right). \tag{4.80}$$

Numerically, we have verified that

$$\phi = -\frac{\pi}{18}. \tag{4.81}$$

Therefore, we find that the quantization condition, at leading order, is

$$\cos\left(\pi \left(\frac{11}{36} - \frac{25E^2}{24\pi^2} \right) \right) = 0, \tag{4.82}$$

which is precisely what one obtains from (4.75) and (4.76) when $\hbar = 2\pi$. We find it remarkable that the argument of the theta function (4.80) is rational and has the right value to reproduce the next-to-leading WKB quantization condition. Of course, one can check explicitly that the zeroes of the theta function (4.73) give the spectrum of $\rho_{3,1}$ for $\hbar = 2\pi$ with very high precision.

The quantization condition encoded in the theta functions (4.71) and (4.73) has a nice interpretation in terms of complex instantons. As we have seen in the example of (4.73), which corresponds to the operator $\rho_{3,1}$ this condition is given, at leading order, by (4.79). The perturbative part of this quantization condition involves the combination of B-periods appearing in υ_2,

$$-\Pi_{B_1} + 2\Pi_{B_2}. \tag{4.83}$$

This follows from (3.30) and the matrix (4.13). The B-cycle (4.83) has a very concrete incarnation as the boundary of the region

$$\mathcal{R}(E) = \{(x, y) \in \mathbb{R}^2 : \mathcal{O}_{3,1}(x, y) \leq \mathrm{e}^E\}, \tag{4.84}$$

which is shown in the left-hand side of Fig. 6 (for $E = 3$). As in [6,10], υ_2 also involves corrections coming from complex instantons associated with the dual A-period. However, there are further subleading corrections involving the other handle of the Riemann surface. These are due to complex instantons associated with other combinations of A- and B-periods. The effects of these instantons are encoded in the genus two theta function, through the dependence in for example υ_1, which involves

$$3\Pi_{B_1} - \Pi_{B_2}. \tag{4.85}$$

This is in agreement with the principle put forward in [49,50]: in a exact WKB analysis, all periods appearing in the complexified Hamiltonian contribute to the quantization condition. This is illustrated in the right-hand side Fig. 6, which shows the underlying genus two curve and its "hidden" cycles. One remarkable implication of our conjecture (3.24) is that all these complex instanton effects are encoded in the higher genus theta function (or a deformation thereof, for general values of $\hbar$).

The vanishing locus of the spectral determinant contains as well information about the perturbed operators O_1, O_2 which are obtained by quantizing the functions (2.34). Let us consider, for example, the operator O_2, which is a perturbation of the operator $\mathsf{O}_{3,1}$. Given a value of the perturbation, $x_0 \geq 0$,

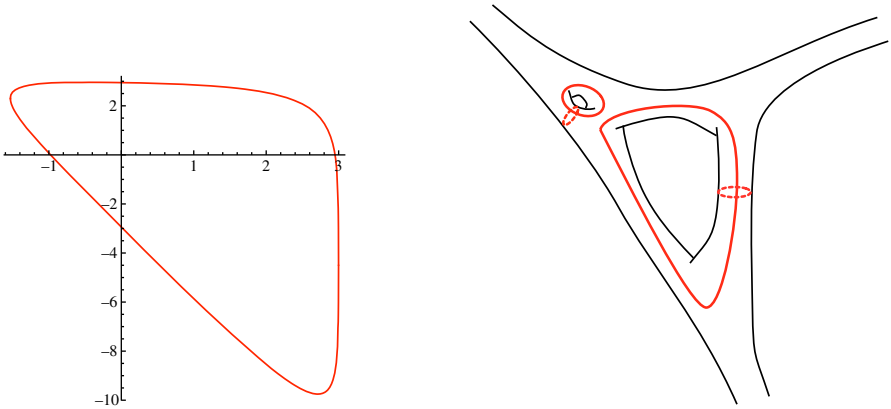

FIGURE 6. *On the right-hand side* we show the boundary of the region (4.84). This is the B-cycle which leads to the perturbative WKB quantization condition. However, when we consider the full complexified genus two curve, we find other cycles which correspond to complex instantons and also contribute to the quantization condition

TABLE 3. The ground-state and first excited energies, E_0 and E_1, for the perturbed $\rho_{3,1}$ operator, as obtained from the vanishing locus of the spectral determinant $\Xi(20, x_3; 2\pi)$

Order	E_0	E_1
4	3.1223827669081676	4.233804854297745
6	3.1220388008498759	4.286273969753037
9	3.1220387541932648	4.286366387547196
12	3.1220387541932659	4.286366387477153
Numerical value	3.1220387541932659	4.286366387477153

This is a power series around $x_3 = 0$, and to obtain the energies we truncate it at a given order in x_3. As we keep more and more terms in the series, we quickly approach the energy obtained by numerical methods

the conjecture predicts the spectrum as follows. We look at the values of x_3 such that $\Xi(x_0, x_3^{(n)}; 2\pi)$ vanishes. The spectrum of O_2, for the given value of x_0, is then

$$\left\{-\mathrm{e}^{E_n}\right\}_{n=0,1,\ldots} = \left\{x_3^{(n)} : \Xi\left(x_0, x_3^{(n)}; 2\pi\right) = 0\right\}. \tag{4.86}$$

Graphically, these values are obtained by taking the intersection of the curves in Fig. 5 with the vertical line $x_0 =$ constant. The predictions can be compared by the spectrum obtained by numerical diagonalization. We find an excellent agreement, as we show for $x_0 = 20$ in Table 3. Of course, completely similar considerations apply to the perturbed operator O_1.

The vanishing locus of the spectral determinant determines also the spectrum of the operator

$$\mathsf{O}_{1,1} + x_4 \mathrm{e}^{2\mathsf{x}}, \tag{4.87}$$

which is obtained by quantization of the mirror curve in the form (4.9). This is a perturbation of the operator $\mathsf{O}_{1,1}$, which is obtained by quantizing the mirror curve to local $\mathbb{P}^2$. To determine the spectrum, we proceed as follows. Given a value of the perturbation x_4, we have a corresponding value of x_3 given by

$$x_3 = x_4^{-3/5}. \tag{4.88}$$

This automatically determines an infinite, discrete series of (negative) values of x_0, $x_0^{(n)}$, $n = 0, 1, \ldots$, in the vanishing locus of the spectral determinant. Then the energy levels of the operator (4.87) are determined by

$$-\mathrm{e}^{E_n} = x_4^{1/5} x_0^{(n)}, \qquad n = 0, 1, \ldots \tag{4.89}$$

We find again an excellent agreement between the numerical spectrum, as obtained by diagonalization of (4.87), and the one predicted by (4.89).

In Fig. 7, we illustrate these considerations for different cases. The dots indicate the spectrum as computed numerically by diagonalization of the operators. The vertical group of dots in the fourth quadrant corresponds to a perturbed operator O_2 with $x_0 = 300$. The horizontal group of dots at the top of the second quadrant corresponds to a perturbation of the operator O_1 with $x_3 = 500$. Finally, the horizontal group of dots at the bottom of the second quadrant corresponds to the perturbed operator $\mathsf{O}_{1,1}$ with $x_4 = 6^{-5}$. In all cases, we find perfect agreement between the numerical results and the prediction from the vanishing locus.

It turns out that one can also consider negative values of the perturbations. For example, one can consider $x_0 < 0$ for the operator O_2 in (4.23). The generalized spectral determinant predicts that, in this case, the values of $x_3^{(n)} = -\mathrm{e}^{E_n}$ for the first eigenstates will be positive, while the remaining values will be negative. This is easy to understand from the explicit expression in (4.23): the operator $\mathsf{O}_{3,1}$ gives positive contributions to the exponentiated energy, while the perturbation gives a negative contribution. For the low-lying eigenstates, the perturbation takes over, while for the higher, excited states, the operator $\mathsf{O}_{3,1}$ takes over. An example of such a situation is shown in Fig. 8, for $x_0 = -300$. Again, the predictions are in perfect agreement with the numerical results.

4.4. The Large N Limit of Spectral Traces

As we explained in Sect. 3.3, the generalized spectral determinant provides a non-perturbative completion of the conventional topological string free energy. The genus expansion of the topological string, in the frame associated with the maximal conifold locus, appears as an asymptotic expansion of the fermionic spectral traces $Z_X(\boldsymbol{N}, \hbar)$. This is, however, a non-trivial statement, since it is based on the conjecture that the non-perturbative corrections to the spectral

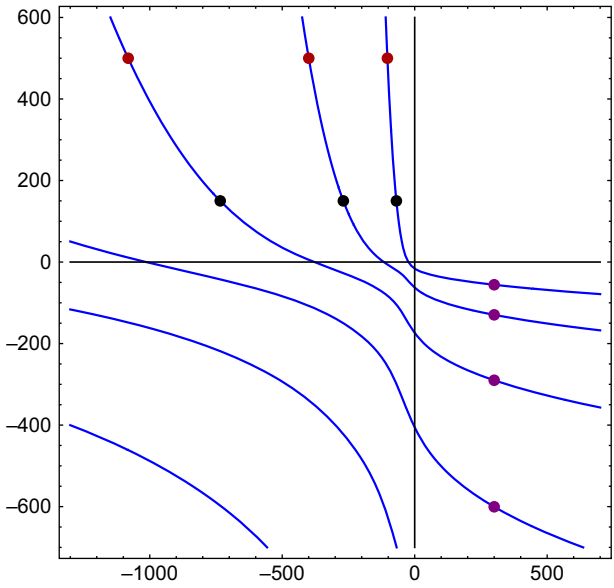

FIGURE 7. The *blue lines* represent the locus in the (x_0, x_3) plane where the spectral determinant (4.38) vanishes. The *horizontal group of dots* in *red* in the second quadrant represents the points $(x_0^{(n)}, x_3) = (-\mathrm{e}^{E_n}, 500)$, $n = 0, 1, 2$, which give the spectrum of the operator O_1 for the value $x_3 = 500$. The *vertical group of dots* in *purple*, in the fourth quadrant, represents the points $(x_0, x_3^{(n)}) = (300, -\mathrm{e}^{E_n})$, $n = 0, 1, 2, 3$, giving the spectrum of the operator O_2 with $x_0 = 300$. Finally, the *horizontal group of dots* in *black*, in the second quadrant, represents the points $(x_0^{(n)}, x_3) = (-\mathrm{e}^{E_n} 6, 6^3)$, which encode the spectrum of the perturbed $\mathbb{P}^2$ operator (4.87) with $x_4 = 6^{-5}$ (color figure online)

problem are encoded in the conventional topological string. It was pointed out in [12,13] that this statement can be, however, checked if one can expand the spectral traces in the strong coupling limit $\hbar \to \infty$. One can then compare this expansion with the predictions of the topological string. We will now perform such a comparison.

Let us first calculate the asymptotic expansion (1.2) directly on the operator side. In our case, this reads

$$\log Z(N_1, N_2; \hbar) = \hbar^2 \mathcal{F}_0(\lambda_1, \lambda_2) + \mathcal{F}_1(\lambda_1, \lambda_2) + \cdots \tag{4.90}$$

We note that, when $N_2 = 0$ or $N_1 = 0$, the l.h.s. reduces to the fermionic spectral trace of the operators $\rho_{2,2}$ or $\rho_{3,1}$, respectively. It follows that

$$\mathcal{F}_g(\lambda_1, \lambda_2) = \mathcal{F}_g^{(2,2)}(\lambda_1) + \mathcal{F}_g^{(3,1)}(\lambda_2) + \mathcal{O}(\lambda_1 \lambda_2)\,. \tag{4.91}$$

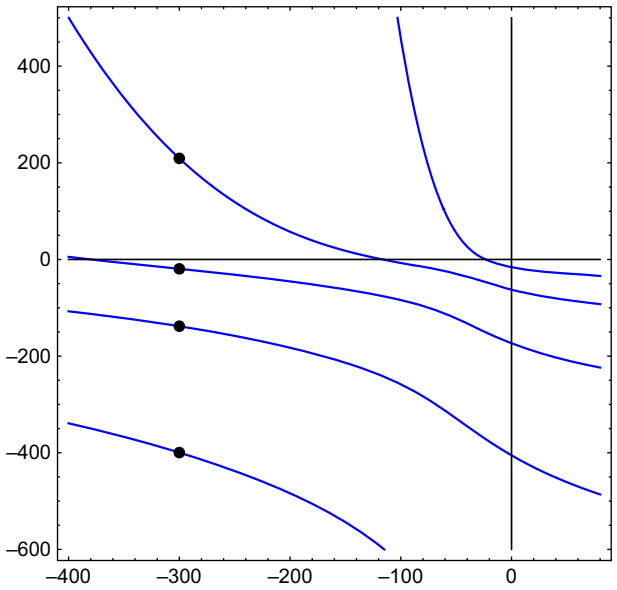

FIGURE 8. The *dots* represent the points $(x_0, x_3^{(n)}) = (-300, -\mathrm{e}^{E_n})$, $n = 1, 2, 3, 4$, giving the spectrum of the operator O_2 with a negative value of $x_0 = -300$

The expansions of $\mathcal{F}_g^{(2,2)}(\lambda)$ and $\mathcal{F}_g^{(3,1)}(\lambda)$ near $\lambda = 0$ were worked out in [12], for small g, and directly from the spectral theory. One finds, for the leading terms,

$$\begin{aligned}\mathcal{F}_0^{(2,2)}(\lambda) &= \frac{\lambda^2}{2}\left(\log(\lambda\sigma_1) - \frac{3}{2}\right) - c_1\lambda - \frac{1}{75}\sqrt{65 - 22\sqrt{5}}\pi^2\lambda^3 \\ &\quad - \frac{\left(174\sqrt{5} - 425\right)\pi^4\lambda^4}{11250} + \frac{4\left(145 - 59\sqrt{5}\right)\sqrt{5 - 2\sqrt{5}}\pi^6\lambda^5}{46875} \\ &\quad + \mathcal{O}(\lambda^6), \\ \mathcal{F}_0^{(3,1)}(\lambda) &= \frac{\lambda^2}{2}\left(\log(\lambda\sigma_2) - \frac{3}{2}\right) - c_2\lambda - \frac{1}{75}\sqrt{65 + 22\sqrt{5}}\pi^2\lambda^3 \\ &\quad + \frac{\left(425 + 174\sqrt{5}\right)\pi^4\lambda^4}{11250} - \frac{4\sqrt{14530 + \frac{32482}{\sqrt{5}}}\pi^6\lambda^5}{9375} + \mathcal{O}(\lambda^6). \end{aligned} \tag{4.92}$$

In these equations,

$$\sigma_1 = \frac{2}{25}\sqrt{10 - 2\sqrt{5}}\pi^2, \qquad \sigma_2 = \frac{2}{25}\sqrt{10 + 2\sqrt{5}}\pi^2. \tag{4.93}$$

The coefficients $c_{1,2}$ can be expressed in terms of the Bloch–Wigner function,

$$D_2(z) = \mathrm{Im}\left(\mathrm{Li}_2(z)\right) + \log|z|\arg(1 - z), \tag{4.94}$$

where arg denotes the branch of the argument between $-\pi$ and π. We have

$$c_1 = \frac{5}{2\pi^2} D_2\left(\mathrm{e}^{\frac{2\pi \mathrm{i}}{5}} \frac{1+\sqrt{5}}{2}\right), \qquad c_2 = \frac{5}{2\pi^2} D_2\left(\mathrm{e}^{\frac{\pi \mathrm{i}}{5}} \frac{1+\sqrt{5}}{2}\right). \tag{4.95}$$

For the next-to-leading function, one finds,

$$\begin{aligned}
\mathcal{F}_1^{(2,2)}(\lambda) &= -\frac{1}{12}\log(\lambda\hbar) + \zeta'(-1) + \frac{\sqrt{725-178\sqrt{5}}\pi^2}{150}\,\lambda \\
&\quad + \frac{\left(174\sqrt{5}-425\right)\pi^4}{11250}\,\lambda^2 - \frac{4\sqrt{112450-\frac{249538}{\sqrt{5}}}\pi^6}{28125}\,\lambda^3 + \mathcal{O}(\lambda^4), \\
\mathcal{F}_1^{(3,1)}(\lambda) &= -\frac{1}{12}\log(\lambda\hbar) + \zeta'(-1) + \frac{\sqrt{725+178\sqrt{5}}\pi^2}{150}\,\lambda \\
&\quad - \frac{\left(425+174\sqrt{5}\right)\pi^4}{11250}\,\lambda^2 + \frac{4\sqrt{112450+\frac{249538}{\sqrt{5}}}\pi^6}{28125}\,\lambda^3 + \mathcal{O}(\lambda^4).
\end{aligned} \tag{4.96}$$

The results above do not determine the crossing terms. To obtain these, we have to calculate fermionic traces with both N_1, N_2 different from zero, and expand them at large $\hbar$. These expansions can be obtained, as in [12,13], by writing integral expressions for the traces and expanding them around the Gaussian point. For example, for the calculation of $Z(1,1;\hbar)$ we need the integral expression (4.50), and we obtain

$$\begin{aligned}
\log Z(1,1;\hbar) &= \frac{1}{2}\log\left[\frac{2\left(7\sqrt{5}-15\right)\pi^2}{625\hbar^2}\right] - c_1 - c_2 + \frac{\sqrt{\frac{1}{2}\left(1205+31\sqrt{5}\right)}\pi^2}{75\hbar} \\
&\quad - \frac{8\left(\left(5+11\sqrt{5}\right)\pi^4\right)}{625\hbar^2} + \cdots .
\end{aligned} \tag{4.97}$$

We have examined the very first terms in the large $\hbar$ expansion of $Z(1,1;\hbar)$, $Z(2,1;\hbar)$ and $Z(1,2;\hbar)$, which allows us to determine the coefficients of the cross terms $\lambda_1\lambda_2$, $\lambda_1^2\lambda_2$, $\lambda_1\lambda_2^2$ in $\mathcal{F}_0(\lambda_1,\lambda_2)$. In this way, we find

$$\begin{aligned}
\mathcal{F}_0(\lambda_1,\lambda_2) &= \mathcal{F}_0^{(2,2)}(\lambda_1) + \mathcal{F}_0^{(3,1)}(\lambda_2) + \alpha_{12}\lambda_1\lambda_2 \\
&\quad + \frac{4}{25}\sqrt{5+2\sqrt{5}}\pi^2\lambda_1\lambda_2^2 + \frac{4}{25}\sqrt{5-2\sqrt{5}}\pi^2\lambda_1^2\lambda_2 + \cdots
\end{aligned} \tag{4.98}$$

where

$$\alpha_{12} = -\log\left[\frac{3+\sqrt{5}}{2}\right]. \tag{4.99}$$

Note that, in comparing an expansion at small N_1, N_2 like (4.97) to (4.92), (4.96), we cannot use the asymptotic expansion of the Barnes functions $G_2(N_1+1)$, $G_2(N_2+1)$, which give the very first terms in (4.92), (4.96). Rather, we have to subtract these terms from the asymptotic expansion, and replace them by the exact values of the Barnes functions, similar to what was done in [69] in a related context.

We now want to compare these results with the predictions of (3.35). According to (3.42), the 't Hooft parameters are given by

$$\lambda_1 = \frac{1}{8\pi^3}\left(3\frac{\partial \widehat{F}_0}{\partial t_1} - \frac{\partial \widehat{F}_0}{\partial t_2} - \frac{\pi^2}{2}\right),$$
$$\lambda_2 = \frac{1}{8\pi^3}\left(-\frac{\partial \widehat{F}_0}{\partial t_1} + 2\frac{\partial \widehat{F}_0}{\partial t_2} - \frac{2\pi^2}{3}\right). \tag{4.100}$$

We recall that the prepotential $\widehat{F}_0(t_1, t_2)$ appearing here is the standard large radius prepotential of this geometry, but after turning on the B-field (4.30). As in the genus one case, we expect the λ_i to be vanishing flat coordinates around the point in the conifold locus characterized by two vanishing periods. The natural candidate is the maximal conifold point (4.8). In Appendix A.3 we have found flat coordinates $t^c_{1,2}$ around this point by solving the Picard–Fuchs equations. Note, however, that we have to turn on a B-field, which is equivalent to changing $z_1 \to -z_1$ in the results of that Appendix. We will keep the same notation for the resulting flat coordinates after this change of sign. A detailed numerical analysis shows that indeed

$$t^c_i = r_i \lambda_i, \qquad i = 1, 2, \tag{4.101}$$

where

$$r_1 = 4\pi^2\sqrt{1 - \frac{2}{\sqrt{5}}}, \qquad r_2 = 4\pi^2\sqrt{1 + \frac{2}{\sqrt{5}}}. \tag{4.102}$$

As we noted in Sect. 3.3, the constants in (4.100) are determined by the coefficients b_i^{NS} and the matrix (4.13). It was observed in the Appendix to [28] that the combinations appearing in (4.100) are precisely vanishing flat coordinates along the two different branches of the conifold locus which intersect at the maximal conifold point. Interestingly, we can predict these combinations from our main conjecture (3.24), as it has been already noted in [13].

According to (3.44), the leading term in the expansion (1.2) is determined by the equations,

$$\frac{\partial \mathcal{F}_0}{\partial \lambda_1} = \frac{1}{10\pi}\Pi^-_v, \qquad \frac{\partial \mathcal{F}_0}{\partial \lambda_2} = \frac{1}{10\pi}\Pi^-_u, \tag{4.103}$$

where $\Pi^-_{v,u}$ are the combinations of A-periods written down in (A.9), (A.10), but after changing $z_1 \to -z_1$ in the power series expansion. To integrate these equations and expand them around $\lambda_1 = \lambda_2 = 0$, so as to make contact with the expansions of the spectral traces, we have to consider the analytic continuation of the periods $\Pi^-_{v,u}$ around the maximal conifold point, i.e., we have to express them as a linear combination of the flat coordinates $\lambda_{1,2}$ and the logarithmic periods $S_{1,2}$ in (A.38). This seems to be difficult, analytically. However, our conjecture *predicts* that this combination should be

$$\frac{1}{10\pi}\Pi_v^- = \frac{1}{r_1}S_1 + \left(\log\frac{\sigma_1}{r_1} - 1\right)\lambda_1 - c_1 + \alpha_{12}\lambda_2,$$
$$\frac{1}{10\pi}\Pi_u^- = \frac{1}{r_2}S_2 + \left(\log\frac{\sigma_2}{r_2} - 1\right)\lambda_2 - c_2 + \alpha_{12}\lambda_1, \tag{4.104}$$

where α_{12}, given in (4.99), is the coefficient of $\lambda_1\lambda_2$ in $\mathcal{F}_0(\lambda_1,\lambda_2)$. We have verified (4.104) numerically. In particular, a remarkable consequence of (4.104) is the following. Let us write (A.10) as

$$\Pi_u(z_1,z_2) = \log(z_1 z_2^3) + \widetilde{\Pi}_u(z_1,z_2),$$
$$\Pi_v(z_1,z_2) = \log(z_1^2 z_2) + \widetilde{\Pi}_v(z_1,z_2). \tag{4.105}$$

Then, if we denote the coordinates of the maximal conifold point (4.8) as $z_{1,2}^c$, we find, by evaluating (4.104) at $(-z_1^c, z_2^c)$, that

$$-\frac{1}{25}\left(\log\left|z_1^c(z_2^c)^3\right| + \widetilde{\Pi}_u(z_1^c,z_2^c)\right) = \frac{1}{\pi}D_2\left(\mathrm{e}^{\frac{\pi\mathrm{i}}{5}}\frac{1+\sqrt{5}}{2}\right),$$
$$-\frac{1}{25}\left(\log\left|(z_1^c)^2 z_2^c\right| + \widetilde{\Pi}_v(z_1^c,z_2^c)\right) = \frac{1}{\pi}D_2\left(\mathrm{e}^{\frac{2\pi\mathrm{i}}{5}}\frac{1+\sqrt{5}}{2}\right), \tag{4.106}$$

where we took into account the expressions (4.95). Similar identities, evaluating the A-periods at the conifold point in terms of the dilogarithm function, were already predicted by the conjecture of [1] in the genus one case, as explained in [12,13]. For elliptic mirror curves, some of these identities have been known in the mathematics and physics literature [15,16,70]. In our approach, these identities follow from the presence of the *quantum* dilogarithm in the integral kernel of the corresponding operators [11]. As already emphasized in [12,13], the fact that these identities are true is a highly non-trivial test of the spectral theory/mirror symmetry correspondence of [1] that we are developing in this paper for the higher genus case. In particular, the identities (4.106), which we have verified with high numerical precision, do not seem to be known in the mathematics literature.[3]

Once (4.104) has been established, we can integrate it to obtain, up to a constant,

$$\begin{aligned}\mathcal{F}_0(\lambda_1,\lambda_2) = {}& \frac{\lambda_1^2}{2}\left(\log(\lambda_1\sigma_1) - \frac{3}{2}\right) - c_1\lambda_1 \\ & + \frac{\lambda_2^2}{2}\left(\log(\lambda_2\sigma_2) - \frac{3}{2}\right) - c_2\lambda_2 + \alpha_{12}\lambda_1\lambda_2 \\ & - \frac{1}{75}\sqrt{65-22\sqrt{5}}\pi^2\lambda_1^3 + \frac{4}{25}\sqrt{5+2\sqrt{5}}\pi^2\lambda_2^2\lambda_1 \\ & + \frac{4}{25}\sqrt{5-2\sqrt{5}}\pi^2\lambda_2\lambda_1^2\end{aligned}$$

[3] After the first version of this paper appeared, Charles Doran and Matt Kerr proved these identities using the techniques of [16].

$$
\begin{aligned}
&- \frac{1}{75}\sqrt{65+22\sqrt{5}}\pi^2\lambda_2^3 + \frac{\left(425-174\sqrt{5}\right)\pi^4\lambda_1^4}{11250} \\
&- \frac{32\left(15+7\sqrt{5}\right)\pi^4\lambda_2^3\lambda_1}{1875} \\
&- \frac{8}{125}\pi^4\lambda_1^2\lambda_2^2 - \frac{32\left(-15+7\sqrt{5}\right)\pi^4\lambda_2\lambda_1^3}{1875} \\
&+ \frac{\left(425+174\sqrt{5}\right)\pi^4\lambda_2^4}{11250} + \mathcal{O}(\lambda^5).
\end{aligned} \tag{4.107}
$$

As in the case of mirror curves of genus one, (3.35) predicts that $\mathcal{F}_1(\lambda_1,\lambda_2)$ is given, up to an additive constant, by the genus one free energy in the maximal conifold frame. We can now use (4.18) and the mirror map near the maximal conifold point to obtain, up to an additive constant,

$$
\begin{aligned}
\mathcal{F}_1(\lambda_1,\lambda_2) = &-\frac{1}{12}\log(\lambda_1\lambda_2) + \frac{1}{150}\sqrt{725-178\sqrt{5}}\pi^2\lambda_1 \\
&+ \frac{1}{150}\sqrt{725+178\sqrt{5}}\pi^2\lambda_2 \\
&- \frac{\left(425-174\sqrt{5}\right)\pi^4\lambda_1^2}{11250} + \frac{184\pi^4\lambda_1\lambda_2}{375\sqrt{5}} \\
&- \frac{\left(425+174\sqrt{5}\right)\pi^4\lambda_2^2}{11250} \\
&- \frac{4\sqrt{112450-\frac{249538}{\sqrt{5}}}\pi^6\lambda_1^3}{28125} \\
&- \frac{16\sqrt{35050+\frac{73142}{\sqrt{5}}}\pi^6\lambda_2^2\lambda_1}{9375} \\
&+ \frac{16\sqrt{35050-\frac{73142}{\sqrt{5}}}\pi^6\lambda_2\lambda_1^2}{9375} \\
&+ \frac{4\sqrt{112450+\frac{249538}{\sqrt{5}}}\pi^6\lambda_2^3}{28125} + \mathcal{O}(\lambda^4).
\end{aligned} \tag{4.108}
$$

If we compare the expressions (4.107), (4.108) with the results obtained from spectral theory, we find complete agreement. In particular, the free energies (4.92), (4.96) for the matrix models associated with the operators $\rho_{3,1}$ and $\rho_{2,2}$ are recovered as topological string free energies in the maximal conifold frame, restricted to the two branches $\lambda_1 = 0$, $\lambda_2 = 0$ of the conifold locus, respectively. In addition, one can check that the cross terms (4.107), (4.108) reproduce the expansions of the spectral traces with both N_1 and N_2 different from zero. For example, one finds that the term of order $\hbar^{-2}$ in $\log Z(1,1;\hbar)$, which is the term written down in the second line of (4.97), precisely equals the sum of the coefficients of the quartic terms in $\mathcal{F}_0(\lambda_1,\lambda_2)$, plus the sum of the coefficients of the quadratic terms in $\mathcal{F}_1(\lambda_1,\lambda_2)$.

The conclusion of this rather lengthy and detailed analysis is that the spectral theory associated with the mirror curve of the resolved $\mathbb{C}^3/\mathbb{Z}_5$ orbifold provides a non-perturbative description of topological strings on this toric CY threefold. More precisely, the fermionic spectral traces $Z(N_1, N_2; \hbar)$, which are perfectly well defined, can be expanded in a 't Hooft limit which reproduces the genus expansion of the topological string free energy, as we have verified in detail.

It is also possible to write the expression (2.64) in the form of a two-cut matrix model. To do this, one has to use the explicit expression for the kernels (4.47) as well as the Cauchy identity, similar to what was done in [12,13] for genus one mirror curves. A straightforward calculation shows that the matrix model calculating the spectral trace $Z(N_1, N_2; \hbar)$ is given by

$$\begin{aligned} Z(N_1, N_2; \hbar) = \frac{1}{N_1! N_2!} \int \frac{\mathrm{d}^N u}{(2\pi)^N} \prod_{i=1}^{N_1} \left| \Psi_{\frac{3\mathsf{b}}{10}, \frac{\mathsf{b}}{10}} \left(\frac{\mathsf{b} u_i}{2\pi} \right) \right|^2 \\ \times \prod_{j=1+N_1}^{N_2} \mathrm{e}^{-\frac{\mathsf{b}^2 u_j}{5}} \left| \Psi_{\frac{2\mathsf{b}}{10}, \frac{\mathsf{b}}{10}} \left(\frac{\mathsf{b} u_j}{2\pi} \right) \right|^2 \\ \times \frac{\prod_{i<j} 2\sinh\left(\frac{u_i - u_j}{2} + \mathrm{i}\pi\Delta_{i,j} \right) 2\sinh\left(\frac{u_i - u_j}{2} - \mathrm{i}\pi\Delta_{i,j} \right)}{\prod_{i,j} 2\cosh\left(\frac{u_i - u_j}{2} + \pi \mathrm{i} c_{i,j} \right)}, \end{aligned} \tag{4.109}$$

where

$$\Delta_{i,j} = \begin{cases} 0 & \text{if } i,j \leq N_1 \text{ or } i,j > N_1, \\ 1/10 & \text{if } i \leq N_1 \text{ and } j > N_1, \\ -1/10 & \text{otherwise,} \end{cases} \tag{4.110}$$

and

$$c_{i,j} = \begin{cases} 3/10 & \text{if } i,j \leq N_1, \\ 1/10 & \text{if } i,j \geq N_1, \\ 2/10 & \text{otherwise} \end{cases} \tag{4.111}$$

In principle, our conjecture provides such a matrix model-like description of the topological string for *all* toric CY threefold, and it would be very interesting to test it in more higher genus examples.

5. Conclusions and Future Prospects

In this paper, we have extended the correspondence of [1] to mirror curves of higher genus. This generalization requires many new ingredients: on the spectral theory side, we need a generalized spectral determinant which gives an entire function on the moduli space. This leads to a single quantization condition, in contrast to what happens in many quantum integrable systems.

We have seen that this quantization condition captures in detail the spectrum of the operators appearing in the quantization of the curve. In addition, the fermionic spectral traces, which are obtained by expanding the generalized spectral determinant, provide a non-perturbative definition of the all-genus topological string in a certain conifold frame. All these considerations have been analyzed in detail in the example of the resolved $\mathbb{C}^3/\mathbb{Z}_5$ orbifold.

The results presented in this paper open different avenues for future research. The general theory presented here grew out of a detailed analysis of the resolved $\mathbb{C}^3/\mathbb{Z}_5$ orbifold, and it would be very important to consider other higher genus examples to test it more carefully. It would be also important to extend our checks (which were mostly done in the maximally supersymmetric case) to arbitrary values of $\hbar$. We should note, however, that this seems to require a deeper understanding of the all-genus topological string away from the large radius point. Already in the genus one case, it was noted in [1] that, for example, the expansion of the spectral determinant near orbifold points is only feasible in the maximally supersymmetric case, since we do not have systematic resummations of the topological string amplitudes at those points. In the case of higher genus curves, there are even more limitations of this type. For example, the operators $\rho_{3,1}$ and $\rho_{2,2}$ correspond to half-orbifold points of the geometry, and it seems difficult to write down an explicit quantization condition for these operators in terms of half-orbifold quantities for general $\hbar$. Clearly, more work is needed along this direction.

Another related question is the following. In the case of genus one curves and for general $\hbar$, it has been shown in [77] that the condition for the vanishing of the spectral determinant (i.e., the quantization condition) can be written in a closed form, in terms of the NS free energy (3.13). It would be interesting to see if a similar simple form can be found in the higher genus case. This might be, however, more difficult than for mirror curves of genus one. Recall that, in the maximally supersymmetric case, the quantization condition involves the vanishing of the usual Riemann theta function. When $g_\Sigma \geq 2$, however, the theta divisor has a more complicated parametrization than in genus one, involving in particular the Abel map, and it is not clear that one can write a simple quantization condition even when $\hbar = 2\pi$.

As we have emphasized, the quantization scheme for mirror curves of higher genus that we are proposing in this paper is different from the more conventional procedure based on an underlying quantum integrable system. On the other hand, a construction by Goncharov and Kenyon associates an integrable system with any toric CY manifold [71] (see also [72,73]). The quantization of this system leads to g_Σ quantization conditions for the moduli of the curve. It would be very interesting to understand the precise relation between the quantization of the Goncharov–Kenyon system and the quantization procedure developed here.

The results obtained in this paper might have implications for the study of non-perturbative aspects of Chern–Simons matter theories. Some of the models studied in [74–76] in the Fermi gas approach involve operators which

are obtained from the quantization of higher genus curves. The methods and ideas developed in this paper should be useful in their study.

Of course, there remain deep conceptual questions concerning the origin of the correspondence between spectral theory and topological strings. From a mathematical point of view, it would be important to develop a version of the complex WKB method which makes it possible to understand the structure of non-perturbative corrections postulated in the conjecture of [1] and the extension studied here. From a physical point of view, it would be important to know whether there is a full-fledged field theory behind the operators obtained by quantization. As pointed out in [1], the behavior of the fermionic spectral traces at large N suggests that it could be a theory of M2 branes. Finding and describing in detail such a theory would lead to a much deeper understanding of topological string theory in the toric case.

Acknowledgements

First of all, we would like to thank Jie Gu, Albrecht Klemm and Jonas Reuter for initial collaboration in this project and for sharing with us some of their results on the resolved $\mathbb{C}^3/\mathbb{Z}_5$ orbifold. We are grateful to Andrea Brini, Charles Doran, Sebastián Franco, Krzysztof Gawedzki, Gian Michele Graf, Yasuyuki Hatsuda, Rinat Kashaev, Matt Kerr and Szabolcs Zakany for useful discussions and correspondence. This work is supported in part by the Fonds National Suisse, subsidies 200021-156995 and 200020-141329, and by the NCCR 51NF40-141869 "The Mathematics of Physics" (SwissMAP).

Appendix A: Special Geometry of the Resolved $\mathbb{C}^3/\mathbb{Z}_5$ Orbifold

In this Appendix, we collect necessary information on the resolved $\mathbb{C}^3/\mathbb{Z}_5$ orbifold, in particular its periods. Many of these results have appeared before, in [27–29].

A.1: Periods at Large Radius

The moduli space of complex structures of this CY is parametrized by the complex variables z_1, z_2 introduced in (2.28). The periods of this geometry are solutions to the Picard–Fuchs equations determined by the following operators [27],

$$\begin{aligned}\mathcal{L}_1 = &-2\Theta_{2,1} + \Theta_{3,0} + z_1(-2\Theta_{0,1} + 3\Theta_{0,2} - \Theta_{0,3} + 6\Theta_{1,0} \\ &- 18\Theta_{1,1} + 9\Theta_{1,2} + 27\Theta_{2,0} - 27\Theta_{2,1} + 27\Theta_{3,0}),\end{aligned} \tag{A.1}$$

$$\mathcal{L}_2 = \Theta_{0,2} - 3\Theta_{1,1} + z_2(-2\Theta_{0,1} - 4\Theta_{0,2} + \Theta_{1,0} + 4\Theta_{1,1} - \Theta_{2,0}), \tag{A.2}$$

$$\begin{aligned}\mathcal{L}_3 = &\Theta_{2,1} + z_1 z_2\,(-2\Theta_{0,2} + 2\Theta_{0,3} + 7\Theta_{1,1} \\ &-13\Theta_{1,2} - 3\Theta_{2,0} + 24\Theta_{2,1} - 9\Theta_{3,0})\,,\end{aligned} \tag{A.3}$$

where $\Theta_{i,j}$ stands for the logarithmic derivative of order i w.r.t. z_1 and of order j w.r.t. z_2. The standard way to solve these equations in the large radius point

(see for example [78]) is to consider the fundamental period $\varpi_0(\rho_1,\rho_2)$, given by

$$\varpi_0(\rho_1,\rho_2)=\sum_{\ell,n\geq 0} \times\frac{\Gamma(\rho_1+1)^2\Gamma(\rho_2+1)\Gamma(\rho_1-2\rho_2+1)\Gamma(-3\rho_1+\rho_2+1)z_1^{\ell+\rho_1}z_2^{k+\rho_2}}{\Gamma(\ell+\rho_1+1)^2\Gamma(k+\rho_2+1)\Gamma(\ell-2k+\rho_1-2\rho_2+1)\Gamma(-3\ell+k-3\rho_1+\rho_2+1)}, \tag{A.4}$$

and take derivatives of this quantity w.r.t. ρ_i, $i=1,2$. We will then define,

$$\begin{aligned}\Pi_{A_i}&=\frac{\partial\varpi_0(\rho_1,\rho_2)}{\partial\rho_i}\Big|_{\rho_1=\rho_2=0},\qquad i=1,2,\\ \Pi_{B_1}&=\left(2\partial_{\rho_1}^2+2\partial_{\rho_1}\partial_{\rho_2}+3\partial_{\rho_2}^2\right)\varpi_0(\rho_1,\rho_2)\big|_{\rho_1=\rho_2=0},\\ \Pi_{B_2}&=\left(\partial_{\rho_1}^2+6\partial_{\rho_1}\partial_{\rho_2}+9\partial_{\rho_2}^2\right)\varpi_0(\rho_1,\rho_2)\big|_{\rho_1=\rho_2=0}.\end{aligned} \tag{A.5}$$

We will also denote

$$\varpi_{ij}=\frac{\partial^2\varpi_0}{\partial\rho_i\partial\rho_j}\Big|_{\rho_1=\rho_2=0}. \tag{A.6}$$

One has, explicitly,

$$\begin{aligned}\Pi_{A_1}&=\log(z_1)-6z_1-z_2+45z_1^2-\frac{3z_2^2}{2}+\cdots,\\ \Pi_{A_2}&=\log(z_2)+2z_1+2z_2-15z_1^2+3z_2^2+\cdots,\\ \Pi_{B_1}&=2\log^2(z_1)+2\log(z_1)\log(z_2)+3\log^2(z_2)+\cdots,\\ \Pi_{B_2}&=\log^2(z_1)+6\log(z_1)\log(z_2)+9\log^2(z_2)+\cdots.\end{aligned} \tag{A.7}$$

In terms of the variables (4.14), we have

$$\begin{aligned}z_1&=Q_1+6Q_1^2+Q_1Q_2+9Q_1^3+10Q_1^2Q_2\\ &\quad+56Q_1^4+26Q_1^3Q_2+4Q_1^2Q_2^2+\cdots,\\ z_2&=Q_2-2Q_1Q_2-2Q_2^2+6Q_1Q_2^2+5Q_1^2Q_2\\ &\quad-3Q_2^3-32Q_1^3Q_2-10Q_1Q_2^3-4Q_2^4+\cdots\end{aligned} \tag{A.8}$$

There are two combinations of the A-periods which play an important rôle, since they can be regarded as the flat coordinates corresponding to the moduli x_3, x_0. They are given by,

$$\Pi_u=\Pi_{A_1}+3\Pi_{A_2},\qquad \Pi_v=2\Pi_{A_1}+\Pi_{A_2}. \tag{A.9}$$

As already noted in [29], their expansions can be written in closed form:

$$\begin{aligned}\Pi_u&=\log u+5\sum_{(m,r)'}^{\infty}\frac{\Gamma(5m+2r)}{\Gamma(1+r)\Gamma(1+3m+r)\Gamma(1+m)^2}(-u)^m z_2^r,\\ \Pi_v&=\log v+5\sum_{(n,r)'}^{\infty}\frac{\Gamma(5n+3r)}{\Gamma(1+r)\Gamma(1+2n+r)^2\Gamma(1+n)}(-v)^n(-z_1)^r.\end{aligned} \tag{A.10}$$

Here, $(m,r)'$ and $(n,r)'$ mean that the corresponding pairs run over non-negative pairs of integers, except $(0,0)$. In the same way, one finds the explicit expression

$$\begin{aligned}\Pi_{B_2} = &-\log^2(u) + 2\Pi_{A_1}\log(u)\\ &+10\sum_{m,r}{}' \frac{5\psi(5m+2r)-2\psi(1+m)-3\psi(1+3m+r)}{\Gamma(1+r)\Gamma(1+m)^2\Gamma(1+3m+r)}\\ &\times\Gamma(5m+2r)(-u)^m z_2^r. \end{aligned} \tag{A.11}$$

A.2: Periods at the (Half)-Orbifold Points

We also need the analytic continuation of these periods to the other significant points in moduli space. Let us first consider the half-orbifold point (4.4). Near this point, z_1 is large but z_2 is small. To perform the analytic continuation, it is convenient to write the fundamental period in the Mellin–Barnes form. One has

$$\begin{aligned}\varpi_0(\rho_1,\rho_2) = &\sum_{k\geq 0}\Gamma(\rho_1+1)^2\Gamma(\rho_2+1)(-1)^{k+1}\sin(\pi(3\rho_1-\rho_2))\\ &\times\Gamma(\rho_1-2\rho_2+1)\Gamma(-3\rho_1+\rho_2+1)\\ &\times\int_{\mathcal{C}}\mathrm{d}t\frac{\Gamma(-t)\Gamma(t+1)\Gamma(-k+3t+3\rho_1-\rho_2)}{\pi\Gamma(k+\rho_2+1)\Gamma(t+\rho_1+1)^2\Gamma(-2k+t+\rho_1-2\rho_2+1)}\\ &\times z_2^{k+\rho_2}z_1^{\rho_1+t}. \end{aligned} \tag{A.12}$$

Here, $\mathcal{C}$ is a contour running parallel to the imaginary axis. By closing the contour on the r.h.s. and picking up the residues at

$$t=\ell,\quad \ell\geq 0 \tag{A.13}$$

we obtain (A.4). But we can close the contour on the l.h.s. and pick up the residues at

$$t=\frac{1}{3}(k-n-3\rho_1+\rho_2),\quad n\geq 0, \tag{A.14}$$

and we have

$$\begin{aligned}\varpi_0(\rho_1,\rho_2) = &\sin(3\pi\rho_1-\pi\rho_2)\sum_{k,n\geq 0}(-1)^{k+n+1}x_0^n X^{\frac{1}{3}(5k+n+5\rho_2)}\\ &\times\csc\left(\frac{1}{3}\pi(k-n-3\rho_1+\rho_2)\right)\\ &\times\frac{\Gamma(\rho_1+1)^2\Gamma(\rho_2+1)\Gamma(\rho_1-2\rho_2+1)\Gamma(-3\rho_1+\rho_2+1)}{3n!\Gamma(k+\rho_2+1)\Gamma\left(\frac{1}{3}(-5k-n-5\rho_2+3)\right)\Gamma\left(\frac{1}{3}(k-n+\rho_2+3)\right)^2}, \end{aligned} \tag{A.15}$$

where we introduced the variable

$$X=\frac{1}{x_3} \tag{A.16}$$

and we used

$$z_2=x_0X^2,\quad z_1=\frac{1}{Xx_0^3}. \tag{A.17}$$

The analytic continuation of the large radius periods is simply obtained by taking the derivatives of $\varpi_0(\rho_1,\rho_2)$ in the form (A.15) as in (A.5). For the A-periods, it is easier to consider the combinations Π_u, Π_v in (A.9). Note that the analytic continuation of the period Π_u is straightforward, and we simply obtain

$$\Pi_u(x_0,X) = 5\log X + 5\sum_{(m,r)'} \frac{\Gamma(5m+2r)}{\Gamma(m+1)^2\Gamma(r+1)\Gamma(3m+r+1)} \times(-1)^m X^{5m+2r} x_0^r. \tag{A.18}$$

The analytic continuation of Π_v gives,

$$\Pi_v(x_0,X) = \frac{5}{3}\log X + \frac{5}{3}\sum_{(p,t)'} \frac{(-1)^t\Gamma\left(\frac{1}{3}(p+5t)\right)}{\Gamma(p+1)\Gamma(t+1)\Gamma\left(\frac{t-p}{3}+1\right)^2} \times(-x_0)^p X^{\frac{1}{3}(p+5t)}. \tag{A.19}$$

We have

$$\begin{aligned}\Pi_{A_1}(x_0,X) &= \frac{3}{5}\Pi_v(x_0,X) - \frac{1}{5}\Pi_u(x_0,X),\\ \Pi_{A_2}(x_0,X) &= \frac{2}{5}\Pi_u(x_0,X) - \frac{1}{5}\Pi_v(x_0,X).\end{aligned} \tag{A.20}$$

It is also useful to consider the following periods,

$$\begin{aligned}\pi_{13}(x_0,X) &= -\frac{\Gamma\left(\frac{2}{3}\right)^2}{\Gamma\left(\frac{1}{3}\right)}\sum_{(p,t)''} \frac{(-1)^t\Gamma\left(\frac{1}{3}(p+5t)\right)}{\Gamma(p+1)\Gamma(t+1)\Gamma\left(\frac{t-p}{3}+1\right)^2} \times(-x_0)^p X^{\frac{1}{3}(p+5t)},\\ \pi_{23}(x_0,X) &= \frac{2\Gamma\left(\frac{1}{3}\right)^2}{\Gamma\left(\frac{2}{3}\right)}\sum_{(p,t)'''} \frac{(-1)^t\Gamma\left(\frac{1}{3}(p+5t)\right)}{\Gamma(p+1)\Gamma(t+1)\Gamma\left(\frac{t-p}{3}+1\right)^2} \times(-x_0)^p X^{\frac{1}{3}(p+5t)},\end{aligned} \tag{A.21}$$

where the sum

$$\sum_{(p,t)''} \tag{A.22}$$

runs over all non-negative integers p,t such that $(p,t)\neq(0,0)$ and $\frac{1}{3}(p+5t)-\frac{1}{3}\in\mathbb{N}$, while

$$\sum_{(p,t)'''} \tag{A.23}$$

runs over all non-negative integers p,t such that $(p,t)\neq(0,0)$ and $\frac{1}{3}(p+5t)-\frac{2}{3}\in\mathbb{N}$. For the B-periods, one similarly finds that Π_{B_2} has a straightforward analytic continuation, while for Π_{B_1} we find

$$\Pi_{B_1}(x_0,X)=\frac{10\pi\Gamma\left(\frac{1}{3}\right)}{3\sqrt{3}\Gamma\left(\frac{2}{3}\right)^2}\pi_{13}(x_0,X)+\frac{5\pi\Gamma\left(\frac{2}{3}\right)}{3\sqrt{3}\Gamma\left(\frac{1}{3}\right)^2}\pi_{23}(x_0,X)$$
$$+\frac{1}{3}\Pi_{B_2}(x_0,X)-\frac{10\pi^2}{9}, \tag{A.24}$$

see [31] for a similar derivation.

A similar calculation can be done for the other half-orbifold point, at $x_3=0$. Let us denote

$$Y=\frac{1}{x_0}. \tag{A.25}$$

It is convenient to consider the large radius period, but after changing the sign of z_2. For this half-orbifold point, the particular combination of A-periods which has an easy analytic continuation is Π_v, and it reads,

$$\Pi_v=5\log Y+5\sum_{(n,r)'}\frac{\Gamma(5n+3r)}{\Gamma(1+r)\Gamma(1+2n+r)^2\Gamma(1+n)}Y^{5n+3r}(-x_3)^r. \tag{A.26}$$

The rest of the periods at large radius can be written as linear combinations of the following series,

$$\pi_{1/2}=-Y^{1/2}\sum_{l,s\geq 0}\frac{\Gamma\left(\frac{1}{2}+2l+s\right)}{\Gamma(2+2s-l)\Gamma(1+l)^2\Gamma\left(\frac{1}{2}+l-s\right)}Y^{2l+s}(-x_3)^{2s+1-l}$$
$$\pi_{3/2}=-Y^{3/2}\sum_{s\geq 0}\sum_{l=0}^{2s+1}\frac{3\Gamma\left(\frac{1}{2}+2l+s\right)}{\Gamma(2+2s-l)\Gamma(1+l)^2\Gamma\left(\frac{1}{2}+l-s\right)}$$
$$\times\left(4\psi(1+l)+\psi(1/2+l-s)-5\psi(1/2-2l-s)\right.$$
$$\left.-4\log(4)\right)Y^{2l+s-1}(-x_3)^{2s+1-l},$$
$$\pi_1=-\sum_{s\geq 1}\sum_{l=0}^{s-1}\frac{2(s-1-l)!(2l+s-1)!}{(2s-l)!\ell!^2}(-1)^{s+l}Y^{2l+s}(-x_3)^{2s-l},$$
$$\widetilde{\Pi}_B=5\sum_{(m,r)'}\frac{\Gamma(5m+3r)}{\Gamma(1+r)\Gamma(1+2m+r)^2\Gamma(1+m)}$$
$$\times\left(4\psi(1+2m+r)+\psi(1+m)-5\psi(5m+3r)\right)Y^{5m+3r}(-x_3)^r. \tag{A.27}$$

One finds,

$$\varpi_{11}=-\frac{25}{4}\log^2(Y)+\frac{5}{2}\log(Y)\left(\pi_{1/2}+\Pi_v\right)$$
$$-2\log(4)\pi_{1/2}-\frac{1}{6}\pi_{3/2}-\frac{1}{2}\widetilde{\Pi}_B+\frac{5}{4}\pi_1+\frac{\pi^2}{3},$$
$$\varpi_{12}=-\frac{5}{2}\log(Y)\pi_{1/2}+\log(16)\pi_{1/2}+\frac{1}{6}\pi_{3/2}-\frac{\pi^2}{3},$$
$$\varpi_{22}=0, \tag{A.28}$$

and we finally obtain the following analytic continuation formulae,

$$\begin{aligned}\Pi_{A_1}(Y,x_3) &= \frac{1}{2}\left(\Pi_v + \pi_{12}\right),\\ \Pi_{A_2}(Y,x_3) &= -\pi_{12},\\ \Pi_{B_1}(Y,x_3) &= 2\varpi_{11} + 2\varpi_{12},\\ \Pi_{B_2}(Y,x_3) &= \varpi_{11} + 6\varpi_{12}.\end{aligned} \tag{A.29}$$

Let us finally consider the analytic continuation near the full orbifold point, $x_3 = x_0 = 0$. After some computations, one finds that the fundamental period becomes

$$\begin{aligned}\varpi_0(\rho_1,\rho_2) = \sum_{k,n} &\frac{(-1)^{k+n}\Gamma(\rho_1+1)\Gamma(\rho_2+1)^2\Gamma(\rho_1-3\rho_2+1)\Gamma(-2\rho_1+\rho_2+1)}{15k!n!\Gamma\left(\frac{1}{5}(-3k-n+5)\right)\Gamma\left(-\frac{k}{5}-\frac{2n}{5}+1\right)^2}\\ &\times\sin(\pi(\rho_1-3\rho_2))g(\rho_1,\rho_2,k,n)x_3^k x_0^n,\end{aligned} \tag{A.30}$$

where

$$\begin{aligned}g(\rho_1,\rho_2,k,n) = &-\sin\left(\frac{1}{3}\pi(n+5\rho_1)\right)\csc\left(\frac{1}{15}\pi(3k+n+5\rho_1)\right)\\ &\times\csc\left(\frac{1}{3}\pi(n-\rho_1+3\rho_2)\right)\\ &-\sin\left(\frac{1}{3}\pi(n+5\rho_1-1)\right)\sec\left(\frac{1}{30}\pi(6k+2n+10\rho_1-5)\right)\\ &\times\csc\left(\frac{1}{3}\pi(-n+\rho_1-3\rho_2+1)\right)\\ &-\sin\left(\frac{1}{3}\pi(n+5\rho_1+1)\right)\sec\left(\frac{1}{30}\pi(6k+2n+10\rho_1+5)\right)\\ &\times\csc\left(\frac{1}{3}\pi(n-\rho_1+3\rho_2+1)\right).\end{aligned} \tag{A.31}$$

Then one can check that

$$\begin{aligned}&\Pi_{A_1}(x_0,x_3)\\ &\quad= -\sum_{m,r}\frac{\pi(-1)^{m+r}\left((-1)^m\csc\left(\frac{1}{5}\pi(2m+r)\right)-3\csc\left(\frac{1}{5}\pi(m+3r)\right)\right)}{5m!r!\Gamma\left(-\frac{m}{5}-\frac{3r}{5}+1\right)\Gamma\left(-\frac{2m}{5}-\frac{r}{5}+1\right)^2}x_0^m x_3^r,\\ &\Pi_{A_2}(x_0,x_3)\\ &\quad= \sum_{m,r}\frac{\pi(-1)^{m+r}\left(2(-1)^m\csc\left(\frac{1}{5}\pi(2m+r)\right)-\csc\left(\frac{1}{5}\pi(m+3r)\right)\right)}{5m!r!\Gamma\left(-\frac{m}{5}-\frac{3r}{5}+1\right)\Gamma\left(-\frac{2m}{5}-\frac{r}{5}+1\right)^2}x_0^m x_3^r.\end{aligned} \tag{A.32}$$

This result can also be obtained with the results of [29]. The B-periods can then be obtained by computing derivatives of (A.30). One finds the closed form expression,

$$\Pi_{B_1}(x_0,x_3) = -\frac{8\pi^2}{3} + \sum_{(m,r)'} \frac{\Gamma\left(\frac{1}{5}(m+2r)\right)^2}{m!\Gamma(r+1)\Gamma\left(-\frac{3m}{5}-\frac{r}{5}+1\right)} x_3^m x_0^r,$$
$$\Pi_{B_2}(x_0,x_3) = -2\pi^2 + \frac{1}{2}\sum_{(m,r)'} \frac{\sec\left(\frac{1}{5}\pi(4r-3m)\right)\Gamma\left(\frac{1}{5}(m+2r)\right)^2}{m!\Gamma(r+1)\Gamma\left(-\frac{3m}{5}-\frac{r}{5}+1\right)} (-x_3)^m x_0^r. \tag{A.33}$$

A.3: Periods at the Maximal Conifold Point

The maximal conifold point is defined by (4.8). Near this point, we have the vanishing coordinates ρ_i, $i = 1, 2$, defined by

$$z_1 = -\frac{1}{25} + \rho_1, \qquad z_2 = \frac{1}{5} + \rho_2. \tag{A.34}$$

We expect to have two flat coordinates t_1^c, t_2^c vanishing at the maximal conifold point, and two periods vanishing like $t_i^c \log t_i^c$. In addition, near the maximal conifold point, we expect the discriminant (4.7) to vanish like

$$\Delta \sim t_1^c t_2^c. \tag{A.35}$$

One can indeed find two solutions of the Picard–Fuchs equations with the required behavior. In terms of these flat coordinates, the local coordinates ρ_i, $i = 1, 2$ are given by the expansions,

$$\rho_1 = \frac{\left(25-11\sqrt{5}\right)t_2^c + \left(25+11\sqrt{5}\right)t_1^c}{250} + \frac{\left(337\sqrt{5}-755\right)(t_2^c)^2 - \left(755+337\sqrt{5}\right)(t_1^c)^2}{2500} + \mathcal{O}\left(t^c\right)^3, \tag{A.36}$$
$$\rho_2 = \frac{t_1^c - t_2^c}{5\sqrt{5}} + \frac{\left(7\sqrt{5}-10\right)(t_2^c)^2 + 10t_1^c t_2^c - \left(10+7\sqrt{5}\right)(t_1^c)^2}{250} + \mathcal{O}\left(t^c\right)^3. \tag{A.37}$$

Similarly, one finds the following solutions to the Picard–Fuchs equations,

$$\begin{aligned} S_1 &= t_1^c \log(t_1^c) - \frac{1}{100}\left(10+\sqrt{5}\right)(t_1^c)^2 \\ &\quad + \frac{2}{25}\left(5-2\sqrt{5}\right)t_1^c t_2^c + \frac{1}{25}\left(5-2\sqrt{5}\right)(t_2^c)^2 + \cdots, \\ S_2 &= t_2^c \log(t_2^c) + \frac{1}{25}\left(5+2\sqrt{5}\right)(t_1^c)^2 \\ &\quad + \frac{2}{25}\left(5+2\sqrt{5}\right)t_1^c t_2^c + \frac{1}{100}\left(-10+\sqrt{5}\right)(t_2^c)^2 + \cdots \end{aligned} \tag{A.38}$$

A.4: Quantum Mirror Map

As in [3,52], the quantum mirror map of the $\mathbb{C}^3/\mathbb{Z}_5$ geometry can be computed directly by quantizing the mirror curve with Weyl's prescription, and solving the resulting difference equation. Let us consider the second function in (2.34). After appropriate rescalings of x, y, we find that the equation $\mathcal{O}_2(x,y)+x_3 = 0$ can be written as

$$\mathrm{e}^x + \mathrm{e}^y + z_1 z_2^3 \mathrm{e}^{-3x-y} + z_2 \mathrm{e}^{-x} + 1 = 0. \tag{A.39}$$

Let us introduce the function

$$V(x) = \frac{\psi(x - \mathrm{i}\hbar)}{\psi(x)}, \tag{A.40}$$

where $\psi(x)$ is a wavefunction in the x-representation. Therefore, the equation

$$\left(\mathrm{e}^{\mathsf{x}} + \mathrm{e}^{\mathsf{y}} + z_1 z_2^3 \mathrm{e}^{-3\mathsf{x}-\mathsf{y}} + z_2 \mathrm{e}^{-\mathsf{x}} + 1\right) |\psi\rangle = 0 \tag{A.41}$$

becomes

$$X + z_2 X^{-1} + 1 + V(X) + \frac{z_1 z_2^3 q^{-3} X^{-3}}{V(q^2 X)} = 0, \tag{A.42}$$

where

$$q = \mathrm{e}^{\mathrm{i}\hbar/2}, \qquad X = \mathrm{e}^{x}. \tag{A.43}$$

We can now solve systematically for $V(X)$ as a power series in z_1, z_2. The quantum A-period is then given by

$$\Pi_u(z_1, z_2; \hbar) = \log u + \widetilde{\Pi}_u(z_1, z_2; \hbar), \tag{A.44}$$

where

$$\widetilde{\Pi}_u(z_1, z_2; \hbar) = -5 \operatorname{Res}_{X=0} \left[\frac{1}{X} \log\left(V(X)\right) \right]. \tag{A.45}$$

We find, at the very first orders,

$$\begin{aligned} \widetilde{\Pi}_u(z_1, z_2; \hbar) = {} & 5z_2 + \frac{15 z_2^2}{2} + \frac{50 z_2^3}{3} \\ & - \frac{5 z_2^3 \left(4\left(q^6 + q^4 + q^2 + 1\right) z_1 - 35 q^3 z_2\right)}{4 q^3} \\ & - \frac{z_2^4 \left(5\left(q^{10} + 7q^8 + 7q^6 + 7q^4 + 7q^2 + 1\right) z_1 - 126 q^5 z_2\right)}{q^5} \\ & + \mathcal{O}(z_i^6). \end{aligned} \tag{A.46}$$

It is easy to check that, when $\hbar \to 0$, we recover the classical Π_u period in (A.10).

We can compute another, independent quantum period by using the representation (4.9) of the geometry. After appropriate rescalings, we can write it as

$$\mathrm{e}^{x} + \mathrm{e}^{y} + z_1 \mathrm{e}^{-x-y} + z_2 \mathrm{e}^{2x} + 1 = 0, \tag{A.47}$$

and following the same procedure we used above, we obtain the equation

$$X + z_2 X^2 + 1 + V(X) + \frac{z_1 q^{-1} X^{-1}}{V(q^2 X)} = 0. \tag{A.48}$$

Solving this, we can obtain the quantum A-period corresponding to Π_{A_2}. Namely, we find

$$\Pi_{A_2}(z_1,z_2;\hbar) = \log u + \widetilde{\Pi}_{A_2}(z_1,z_2;\hbar), \tag{A.49}$$

$$\begin{aligned}\widetilde{\Pi}_{A_2}(z_1,z_2;\hbar) &= \mathrm{Res}_{X=0}\left[\frac{1}{X}\left(\log(V(X)) - 2\log(V(X^{-1}))\right)\right] \\ &= (q+q^{-1})z_1 + 2z_2 + \frac{6q^4 z_2^2 + \left(-2q^8 - 7q^6 - 12q^4 - 7q^2 - 2\right) z_1^2}{2q^4} \\ &\quad + \mathcal{O}(z_i^3).\end{aligned} \tag{A.50}$$

References

[1] Grassi, A., Hatsuda, Y., Mariño, M.: Topological strings from quantum mechanics. arXiv:1410.3382 [hep-th]

[2] Aganagic, M., Dijkgraaf, R., Klemm, A., Mariño, M., Vafa, C.: Topological strings and integrable hierarchies. Commun. Math. Phys. **261**, 451 (2006). arXiv:hep-th/0312085

[3] Aganagic, M., Cheng, M.C.N., Dijkgraaf, R., Krefl, D., Vafa, C.: Quantum geometry of refined topological strings. JHEP **1211**, 019 (2012). arXiv:1105.0630 [hep-th]

[4] Nekrasov, N.A., Shatashvili, S.L.: Quantization of integrable systems and four dimensional gauge theories. arXiv:0908.4052 [hep-th]

[5] Drukker, N., Mariño, M., Putrov, P.: From weak to strong coupling in ABJM theory. Commun. Math. Phys. **306**, 511 (2011). arXiv:1007.3837 [hep-th]

[6] Mariño, M., Putrov, P.: ABJM theory as a Fermi gas. J. Stat. Mech. **1203**, P03001 (2012). arXiv:1110.4066 [hep-th]

[7] Hatsuda, Y., Moriyama, S., Okuyama, K.: Instanton effects in ABJM theory from Fermi gas approach. JHEP **1301**, 158 (2013). arXiv:1211.1251 [hep-th]

[8] Hatsuda, Y., Moriyama, S., Okuyama, K.: Instanton bound states in ABJM theory. JHEP **1305**, 054 (2013). arXiv:1301.5184 [hep-th]

[9] Hatsuda, Y., Mariño, M., Moriyama, S., Okuyama, K.: Non-perturbative effects and the refined topological string. JHEP **1409**, 168 (2014). arXiv:1306.1734 [hep-th]

[10] Kallen, J., Mariño, M.: Instanton effects and quantum spectral curves. Annales Henri Poincaré **17**(5), 1037 (2016). arXiv:1308.6485 [hep-th]

[11] Kashaev, R., Mariño, M.: Operators from mirror curves and the quantum dilogarithm. arXiv:1501.01014 [hep-th]

[12] Mariño, M., Zakany, S.: Matrix models from operators and topological strings. Annales Henri Poincaré **17**(5), 1075 (2016). arXiv:1502.02958 [hep-th]

[13] Kashaev, R., Mariño, M., Zakany, S.: Matrix models from operators and topological strings, 2. arXiv:1505.02243 [hep-th]

[14] Gu, J., Klemm, A., Mariño, M., Reuter, J.: Exact solutions to quantum spectral curves by topological string theory. JHEP **1510**, 025 (2015). arXiv:1506.09176 [hep-th]

[15] Rodriguez Villegas, F.: Modular Mahler measures, I. In: Topics in Number Theory, p. 17. Kluwer Acad. Publ., Dordrecht (1999)

[16] Doran, C., Kerr, M.: Algebraic K-theory of toric hypersurfaces. Commun. Number Theory Phys. **5**, 397 (2011). arXiv:0809.4669 [math.AG]

[17] Katz, S.H., Klemm, A., Vafa, C.: Geometric engineering of quantum field theories. Nucl. Phys. B **497**, 173 (1997). arXiv:hep-th/9609239

[18] Chiang, T.M., Klemm, A., Yau, S.T., Zaslow, E.: Local mirror symmetry: calculations and interpretations. Adv. Theor. Math. Phys. **3**, 495 (1999). arXiv:hep-th/9903053

[19] Witten, E.: Phases of N = 2 theories in two-dimensions. Nucl. Phys. B **403**, 159 (1993). arXiv:hep-th/9301042

[20] Hori, K., Vafa, C.: Mirror symmetry. arXiv:hep-th/0002222

[21] Batyrev, V.V.: Dual polyhedra and mirror symmetry for Calabi–Yau hypersurfaces in toric varieties. J. Alg. Geom. **3**, 493 (1994). arXiv:alg-geom/9310003

[22] Aganagic, M., Klemm, A., Vafa, C.: Disk instantons, mirror symmetry and the duality web. Z. Naturforsch. A **57**, 1 (2002). arXiv:hep-th/0105045

[23] Mariño, M.: Open string amplitudes and large order behavior in topological string theory. JHEP **0803**, 060 (2008). arXiv:hep-th/0612127

[24] Bouchard, V., Klemm, A., Mariño, M., Pasquetti, S.: Remodeling the B-model. Commun. Math. Phys. **287**, 117 (2009). arXiv:0709.1453 [hep-th]

[25] Eynard, B., Orantin, N.: Computation of open Gromov–Witten invariants for toric Calabi–Yau 3-folds by topological recursion, a proof of the BKMP conjecture. Commun. Math. Phys. **337**(2), 483 (2015). arXiv:1205.1103 [math-ph]

[26] Huang, M.X., Klemm, A., Poretschkin, M.: Refined stable pair invariants for E-, M- and $[p, q]$-strings. JHEP **1311**, 112 (2013). arXiv:1308.0619 [hep-th]

[27] Klemm, A., Poretschkin, M., Schimannek, T., Westerholt-Raum, M.: Direct integration for mirror curves of genus two and an almost meromorphic Siegel modular form. arXiv:1502.00557 [hep-th]

[28] De la Ossa, X., Florea, B., Skarke, H.: D-branes on noncompact Calabi–Yau manifolds: K theory and monodromy. Nucl. Phys. B **644**, 170 (2002). arXiv:hep-th/0104254

[29] Mukhopadhyay, S., Ray, K.: Fractional branes on a noncompact orbifold. JHEP **0107**, 007 (2001). arXiv:hep-th/0102146

[30] Karp, R.L.: On the $\mathbb{C}^n/\mathbb{Z}_m$ fractional branes. J. Math. Phys. **50**, 022304 (2009). arXiv:hep-th/0602165

[31] Coates, T.: Wall-crossings in toric Gromov–Witten theory, II: local examples. arXiv:0804.2592 [math.AG]

[32] Simon, B.: Trace Ideals and Their Applications, 2nd edn. American Mathematical Society, Providence (2000)

[33] Simon, B.: Notes on infinite determinants of Hilbert space operators. Adv. Math. **24**, 244 (1977)

[34] Grothendieck, A.: La théorie de Fredholm. Bulletin de la Société Mathématique de France **84**, 319 (1956)

[35] Fredholm, I.: Sur une classe d'équations fonctionnelles. Acta Math. **27**, 365 (1903)

[36] Stessin, M., Yang, R., Zhu, K.: Analyticity of a joint spectrum and a multivariable analytic Fredhom theorem. N. Y. J. Math. **17**, 39 (2011)

[37] Chagouel, I., Stessin, M., Zhu, K.: Geometric spectral theory for compact operators. arXiv:1309.4375

[38] Babelon, O., Bernard, D., Talon, M.: An Introduction to Classical Integrable Systems. Cambridge University Press, Cambridge (2003)

[39] Gutzwiller, M.C.: The quantum mechanical Toda lattice. Ann. Phys. **124**, 347 (1980)

[40] Gutzwiller, M.C.: The quantum mechanical Toda lattice: II. Ann. Phys. **133**, 304 (1981)

[41] Sklyanin, E.K.: The quantum Toda chain. Lect. Notes Phys. **226**, 196 (1985)

[42] Gaudin, M., Pasquier, V.: The periodic Toda chain and a matrix generalization of the Bessel function's recursion relations. J. Phys. A **25**, 5243 (1992)

[43] Kharchev, S., Lebedev, D.: Integral representation for the eigenfunctions of quantum periodic Toda chain. Lett. Math. Phys. **50**, 53 (1999). arXiv:hep-th/9910265

[44] An, D.: Complete set of eigenfunctions of the quantum Toda chain. Lett. Math. Phys. **87**, 209 (2009)

[45] Mironov, A., Morozov, A.: Nekrasov functions and exact Bohr-Zommerfeld integrals. JHEP **1004**, 040 (2010). arXiv:0910.5670 [hep-th]

[46] Mironov, A., Morozov, A.: Nekrasov functions from exact BS periods: the case of SU(N). J. Phys. A **43**, 195401 (2010). arXiv:0911.2396 [hep-th]

[47] Kozlowski, K.K., Teschner, J.: TBA for the Toda chain. arXiv:1006.2906 [math-ph]

[48] Matsuyama, A.: Periodic Toda lattice in quantum mechanics. Ann. Phys. **222**, 300 (1992)

[49] Balian, R., Parisi, G., Voros, A.: Discrepancies from asymptotic series and their relation to complex classical trajectories. Phys. Rev. Lett. **41**, 1141 (1978)

[50] Balian, R., Parisi, G., Voros, A.: Quartic oscillator. In: Feynman Path Integrals. Lecture Notes in Physics, vol. 106, p. 337 (1979)

[51] Huang, M.X.: On gauge theory and topological string in Nekrasov–Shatashvili limit. JHEP **1206**, 152 (2012). arXiv:1205.3652 [hep-th]

[52] Huang, M.X., Klemm, A., Reuter, J., Schiereck, M.: Quantum geometry of del Pezzo surfaces in the Nekrasov–Shatashvili limit. JHEP **1502**, 031 (2015). arXiv:1401.4723 [hep-th]

[53] Bershadsky, M., Cecotti, S., Ooguri, H., Vafa, C.: Kodaira–Spencer theory of gravity and exact results for quantum string amplitudes. Commun. Math. Phys. **165**, 311 (1994). arXiv:hep-th/9309140

[54] Gopakumar, R., Vafa, C.: M theory and topological strings. 2. arXiv:hep-th/9812127

[55] Iqbal, A., Kozcaz, C., Vafa, C.: The refined topological vertex. JHEP **0910**, 069 (2009). arXiv:hep-th/0701156

[56] Choi, J., Katz, S., Klemm, A.: The refined BPS index from stable pair invariants. Commun. Math. Phys. **328**, 903 (2014). arXiv:1210.4403 [hep-th]

[57] Nekrasov, N., Okounkov, A.: Membranes and sheaves. arXiv:1404.2323 [math.AG]

[58] Huang, M.X., Klemm, A.: Direct integration for general Ω backgrounds. Adv. Theor. Math. Phys. **16**(3), 805 (2012). arXiv:1009.1126 [hep-th]

[59] Eynard, B., Mariño, M.: A holomorphic and background independent partition function for matrix models and topological strings. J. Geom. Phys. **61**, 1181 (2011). arXiv:0810.4273 [hep-th]

[60] Aganagic, M., Bouchard, V., Klemm, A.: Topological strings and (almost) modular forms. Commun. Math. Phys. **277**, 771 (2008). arXiv:hep-th/0607100

[61] Hatsuda, Y.: Spectral zeta function and non-perturbative effects in ABJM Fermi-gas. JHEP **1511**, 086 (2015). arXiv:1503.07883 [hep-th]

[62] Faddeev, L.D., Kashaev, R.M.: Quantum dilogarithm. Mod. Phys. Lett. A **9**, 427 (1994). arXiv:hep-th/9310070

[63] Garoufalidis, S., Kashaev, R.: Evaluation of state integrals at rational points. Commun. Number Theor. Phys. **09**(3), 549 (2015). arXiv:1411.6062 [math.GT]

[64] Faddeev, L.D.: Discrete Heisenberg-Weyl group and modular group. Lett. Math. Phys. **34**, 249 (1995). arXiv:hep-th/9504111

[65] Fuji, H., Hirano, S., Moriyama, S.: Summing up all genus free energy of ABJM matrix model. JHEP **1108**, 001 (2011). arXiv:1106.4631 [hep-th]

[66] Alim, M., Yau, S.T., Zhou, J.: Airy equation for the topological string partition function in a scaling limit. Lett. Math. Phys. **106**(6), 719 (2016). arXiv:1506.01375 [hep-th]

[67] Huang, M.X., Wang, X.F.: Topological strings and quantum spectral problems. JHEP **1409**, 150 (2014). arXiv:1406.6178 [hep-th]

[68] Ellegaard Andersen, J., Kashaev, R.: A TQFT from quantum Teichmüller theory. Commun. Math. Phys. **330**, 887 (2014). arXiv:1109.6295 [math.QA]

[69] Mariño, M., Schiappa, R., Weiss, M.: Multi-instantons and multi-cuts. J. Math. Phys. **50**, 052301 (2009). arXiv:0809.2619 [hep-th]

[70] Mohri, K., Onjo, Y., Yang, S.K.: Closed submonodromy problems, local mirror symmetry and branes on orbifolds. Rev. Math. Phys. **13**, 675 (2001). arXiv:hep-th/0009072

[71] Goncharov, A.B., Kenyon, R.: Dimers and cluster integrable systems. arXiv:1107.5588 [math.AG]

[72] Fock, V.V., Marshakov, A.: Loop groups, clusters, dimers and integrable systems. arXiv:1401.1606 [math.AG]

[73] Eager, R., Franco, S., Schaeffer, K.: Dimer models and integrable systems. JHEP **1206**, 106 (2012). arXiv:1107.1244 [hep-th]

[74] Moriyama, S., Nosaka, T.: ABJM membrane instanton from pole cancellation mechanism. Phys. Rev. D **92**(2), 026003 (2015). arXiv:1410.4918 [hep-th]

[75] Moriyama, S., Nosaka, T.: Exact instanton expansion of superconformal Chern–Simons theories from topological strings. JHEP **1505**, 022 (2015). arXiv:1412.6243 [hep-th]

[76] Hatsuda, Y., Honda, M., Okuyama, K.: Large N non-perturbative effects in $\mathcal{N} = 4$ superconformal Chern–Simons theories. JHEP **1509**, 046 (2015). arXiv:1505.07120 [hep-th]

[77] Wang, X., Zhang, G., Huang, M.X.: New exact quantization condition for toric Calabi–Yau geometries. Phys. Rev. Lett. **115**, 121601 (2015). arXiv:1505.05360 [hep-th]

[78] Hosono, S., Klemm, A., Theisen, S.: Lectures on mirror symmetry. Lect. Notes Phys. **436**, 235 (1994). arXiv:hep-th/9403096

Santiago Codesido, Alba Grassi and Marcos Mariño
Département de Physique Théorique et Section de Mathématiques
Université de Genève
1211 Geneva
Switzerland
e-mail: santiago.codesido@unige.ch;
alba.grassi@unige.ch;
marcos.marino@unige.ch

Communicated by B. Pioline.
Received: March 22, 2016.
Accepted: July 26, 2016.